PALEOSOLS OF THE WESTPHALIAN D SYDNEY MINES FORMATION, SYDNEY BASIN, CAPE BRETON, NOVA SCOTIA, CANADA.

Thomas Alexander Tremills

Submitted in Partial Fulfilment of the Requirements

for the Degree of Bachelor of Science, Honours

Dalhousie University, Halifax, Nova Scotia

March, 1992

Dalhousie University

Department of Earth Sciences
Halifax, Nova Scotia
Canada B3H 3J5
(902) 494-2358
FAX (902) 494-6889

DATE April 2, 1992

AUTHOR Thomas Alexander Tremills

TITLE Paleosols of the Westphalian D Sydney Mines Formation, Sydney Basin, Cape Breton, Nova Scotia, Canada

Degree B.Sc. Convocation Spring Year 1992

Permission is herewith granted to Dalhousie University to circulate and to have copied for non-commercial purposes, at its discretion, the above title upon the request of individuals or institutions.

Distribution License

DalSpace requires agreement to this non-exclusive distribution license before your item can appear on DalSpace.

NON-EXCLUSIVE DISTRIBUTION LICENSE

You (the author(s) or copyright owner) grant to Dalhousie University the non-exclusive right to reproduce and distribute your submission worldwide in any medium.

You agree that Dalhousie University may, without changing the content, reformat the submission for the purpose of preservation.

You also agree that Dalhousie University may keep more than one copy of this submission for purposes of security, back-up and preservation.

You agree that the submission is your original work, and that you have the right to grant the rights contained in this license. You also agree that your submission does not, to the best of your knowledge, infringe upon anyone's copyright.

If the submission contains material for which you do not hold copyright, you agree that you have obtained the unrestricted permission of the copyright owner to grant Dalhousie University the rights required by this license, and that such third-party owned material is clearly identified and acknowledged within the text or content of the submission.

If the submission is based upon work that has been sponsored or supported by an agency or organization other than Dalhousie University, you assert that you have fulfilled any right of review or other obligations required by such contract or agreement.

Dalhousie University will clearly identify your name(s) as the author(s) or owner(s) of the submission, and will not make any alteration to the content of the files that you have submitted.

If you have questions regarding this license please contact the repository manager at dalspace@dal.ca.

Grant the distribution license by signing and dating below.

_____ _____

Name of signatory Date

ABSTRACT

Lacustrine-deltaic deposits in the Sydney Mines Formation contain paleosols. Three soil profiles (1 m, 1.1 m, and 0.9 m long) sampled over an 11.8 m interval of drill core taken ca. 200 m offshore Point Aconi, Cape Breton, show typical and diagnostic mottled colouring, root traces, plant fossils, and carbonate concretions. The three paleosols are relatively immature, with weakly developed horizonation and relict sedimentary layering. Geochemical evidence (immobile element ratios) indicate that parent materials were inhomogenous and not fully mixed during pedogenesis. Grey colour, and the presence of pyrite, siderite, kutnahorite (Mn-calcite), and organic material indicate the hydromorphic and reducing conditions associated with the pedogenic environment. A thin coal caps one profile.

Electron microprobe analysis of concretions reveals alternate layers of siderite, calcite, kutnahorite, and pyrite. Fluctuations in pH and Eh and limited ion availability probably formed the layers.

The Late Paleozoic Sydney Basin shows repeated sea level fluctuations (cyclothems). The incipient paleosols of this study mark the transition from a high stand (peat marsh and lake deposition) to a low stand (alluvial plain).

Keywords: Sydney Mines Formation, paleosols, root traces, concretions, hydromorphic, cyclothems.

Table of Contents

LIST OF FIGURES

LIST OF TABLES

LIST OF PLATES

ACKNOWLEDGEMENTS

I would like to thank my supervisor, Dr. Martin Gibling, for guidence, encouragement, and financial support in the completion of this thesis, and Robert Naylor who provided invaluable information on the Sydney Basin as well as help with the core log. Bob MacKay helped me with the microprobe enigma, and thanks goes to Patricia Stoffyn for SEM work, and Sally Stanford for producing and advising on XRF data. My fellow honours students were a constant motivating force, and Dr. Clarke always responded with support and advice. And everyone appreciated the sandwiches brought by Paul Stiven.

CHAPTER 1 INTRODUCTION

1.1 Introduction

Paleosols are soils that formed on an ancient landscape (Valentine and Dalrymple 1976). Paleosols are an important lithotype because they signify the former subaerial exposure of an area. However, with detailed analysis they can reveal considerable information concerning paleoclimate (Yaalon 1990), paleogeomorphology (McFarlane 1983), time resolution (Kraus and Bown 1986), basin development (Allen 1974), and porosity evolution of subaerial limestones (Wright 1988). Modern and ancient soils commonly contain economic resources such as nickel, aluminum, iron (McFarlane 1983), uranium, and coal (Retallack 1990).

Excellent introductions to the study of paleosols include: Wright (1986), Retallack (1988, 1990), and Catt (1990).

1.2 Purpose

The purpose of this thesis is to describe and interpret a succession of paleosols from the Westphalian D strata of the Sydney Mines Formation in Cape Breton, Nova Scotia, Canada (Fig. 1.1). Detailed analysis of fifteen samples has revealed a history of moderately developed pedogenic diagenesis, including pre-burial carbonate cementation and glaebule development.

The retrieval of fresh drill-core at Point Aconi (Fig. 1.1) provides the opportunity to further the study of paleosols, and

to shed light on the evolution of the Sydney Basin.

1.3 REGIONAL GEOLOGY

The Sydney Mines Formation is the uppermost formation in the Westphalian C to Stephanian Morien Group. The Morien Group is exposed onshore, but is overlain offshore by thick redbeds that may be in part Permian (Hacquebard 1983; Boehner and Giles 1986). Hacquebard (1983) estimated the thickness of the Morien Group to be 1966 m, and the strata may extend as far as offshore eastern Newfoundland (Rust et al. 1987).

Onshore, the Morien Group has gentle folds that follow the main (northeast) fold trend of the Appalachians. Although the Hollow and Cobequid-Chedabucto fault systems form the boundaries of the Sydney Basin, the Morien Group strata were deposited during an apparently quiet tectonic period, and faulting affected sedimentation patterns very little (Ryan et al. 1987).

The Morien Group is a fluvial and lacustrine sequence. Fresh-water shark and lungfish fossils (Masson and Rust 1984), together with coal and tree fossils (Rust et al. 1987), indicate that a fresh-water environment prevailed. However, the presence of brackish-marine foraminifers indicate a marine influence (Wightman et al. 1992).

The Morien Group fines upward from a predominantly sandstone facies to a sandstone-mudstone facies with interspersed beds of coal and limestone. The fining-upward progression suggests that tectonic activity decreased. The source areas had been eroded and

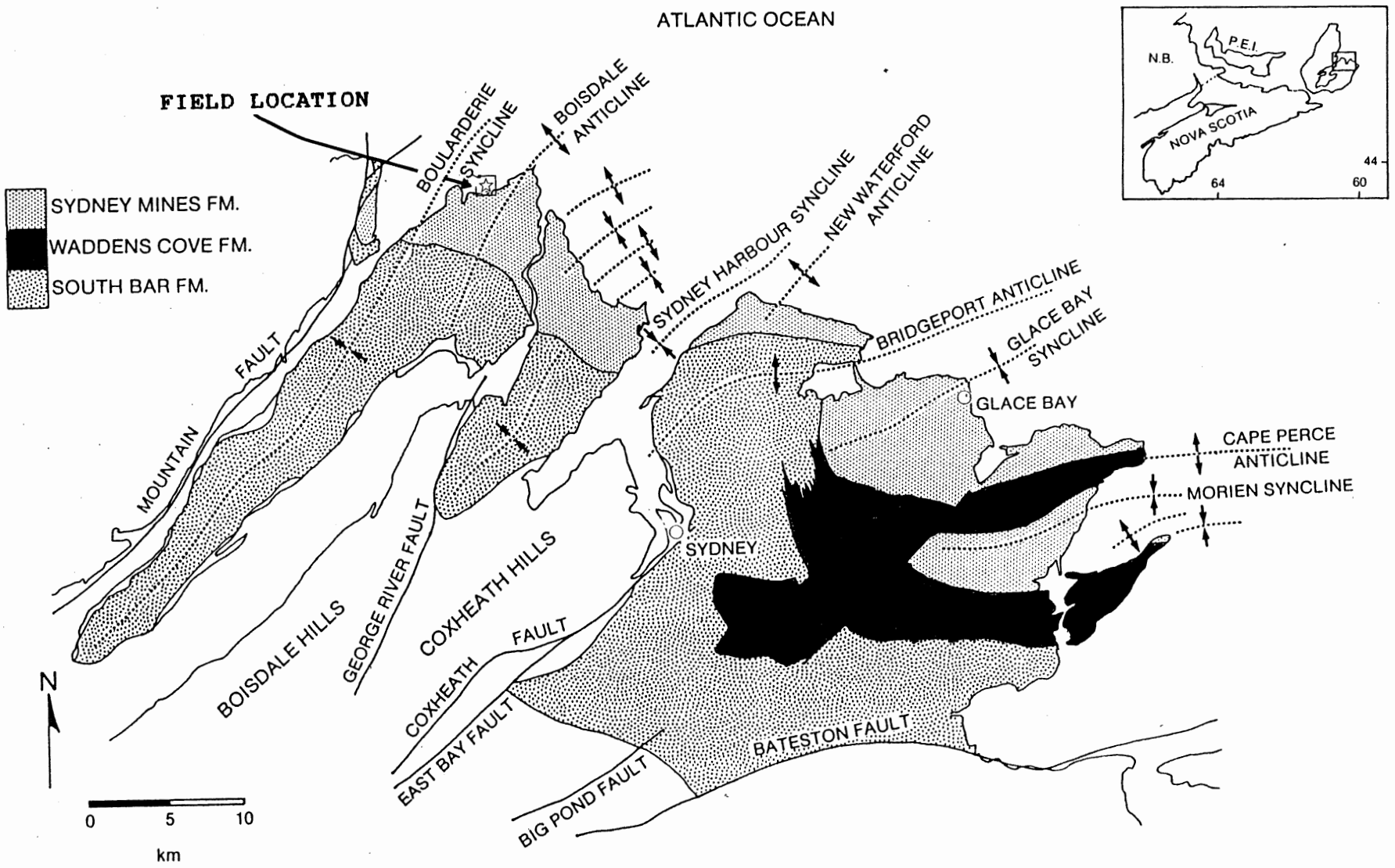

Figure 1.1 Map of eastern Cape Breton with the study area indicated.

basinal subsidence had declined by the time of deposition of the Sydney Mines Formation. The Morien Group comprises three formations from lower to upper they are: the South Bar Formation, the Waddens Cove Formation, and the Sydney Mines Formation.

The South Bar Formation formed in a braided-stream setting. It consists of sandstone with thin, sparse, coals and minor mudstone. This formation covers much of the onshore part of the Sydney Basin (Gibling and Rust 1990).

The Waddens Cove Formation is the lateral equivalent of the upper part of the South Bar Formation. Its strata occur in the southeast part of the Sydney Basin and consist of red mudstones with siliceous paleosols (ganisters)(Rust et al. 1987; Gibling and Rust 1990, in press).

The South Bar Formation passes abruptly upward into strata of the Sydney Mines Formation, consisting of alternate beds of sandstone and mudstone, with limestones and coals. The paleosols of this study developed in a lacustrine delta facies of the Sydney Mines Formation (Masson and Rust 1990).

All formations are coal-bearing; however, only the Sydney Mines Formation contains coals of economic importance (Rust et al. 1987).

1.4 Scope

The paleosols in this study are from one of ten offshore drill holes near Point Aconi (Fig 2.1). The purpose of the drilling was to establish stratigraphic continuity for the

engineering of a fresh-water intake at the future Point Aconi power plant. Using the paleosols as marker beds, R. Naylor of Nova Scotia Department of Natural Resources correlated the stratigraphy over an area of 1 km^2.

The fourteen samples are from core HB-10. The initial core-log indicated the occurrence of paleosols within the strata, and the fourteen samples represent three paleosol profiles that are particularly distinctive.

Analysis of the samples was designed to determine the type and intensity of early diagenesis. Traditionally, descriptions of paleosols have tended to focus on soil macromorphology (observations at outcrop and hand specimen scale). Macromorphology alone, however, provides an inadequate analysis of paleosols. Muhs et al. (1987) and Monger et al. (1991) show the importance of performing more detailed petrological and geochemical analyses of paleosols. Thus, the paleosol descriptions in this study include both macromorphological and micromorphological data. Wright (1986) notes that for identifying paleosols on the basis of soil processes, "micromorphological techniques may prove to be the most useful tools for recognizing and interpreting paleosols".

1.5 Organization

Chapter 2 consists of a core log description and suggests a depositional setting. Chapters 3 and 4 concentrate on petrography and geochemistry, including: bulk chemical analysis by x-ray

fluorescence (XRF), mineral composition analysis by scanning electron microscope (SEM) and electron microprobe (EMP), and mineralogical and textural observations in thin section. Specifically, Chapter 3 presents detailed descriptions of the three profiles using hand sample and thin section data, and Chapter 4 focuses on the geochemistry of the profiles. Chapter 5 presents six main conclusions to summarize the findings of this thesis.

CHAPTER TWO DEPOSITIONAL FRAMEWORK

2.1 Introduction

Core HB-10 (Fig 2.1) was selected for detailed analysis because it contains three particularly distinctive paleosol profiles. This chapter presents a description of the core accompanied by a depositional facies interpretation.

When a soil forms on unconsolidated sediments, deposition and soil development are closely connected. Thus the depositional setting must be understood before interpreting the paleosols.

2.2 Core Description

The following facies interpretations are based on the core log (Figs. 2.2, 2.3) produced by R. Naylor, and use facies modelling by Rust et al. (1987), Walker and Cant (1989), and Tye and Coleman (1989).

The base of the core (at 36.25 m) is a coarse-grained sandstone with large plant fragments and no obvious sedimentary structures. The coarse sandstone fines upwards into a medium-coarse sandstone and exhibits high-angle (trough) cross-stratification and root traces. This basal 6.75 m section represents deposition in a fluvial channel, as indicated by such characteristic features as a basal lag deposit, trough cross-stratification, and upward fining.

At 29.5 m a sharp contact separates the sandstone from a 1.4 m unit of mudstone, interbedded with thin beds of parallel

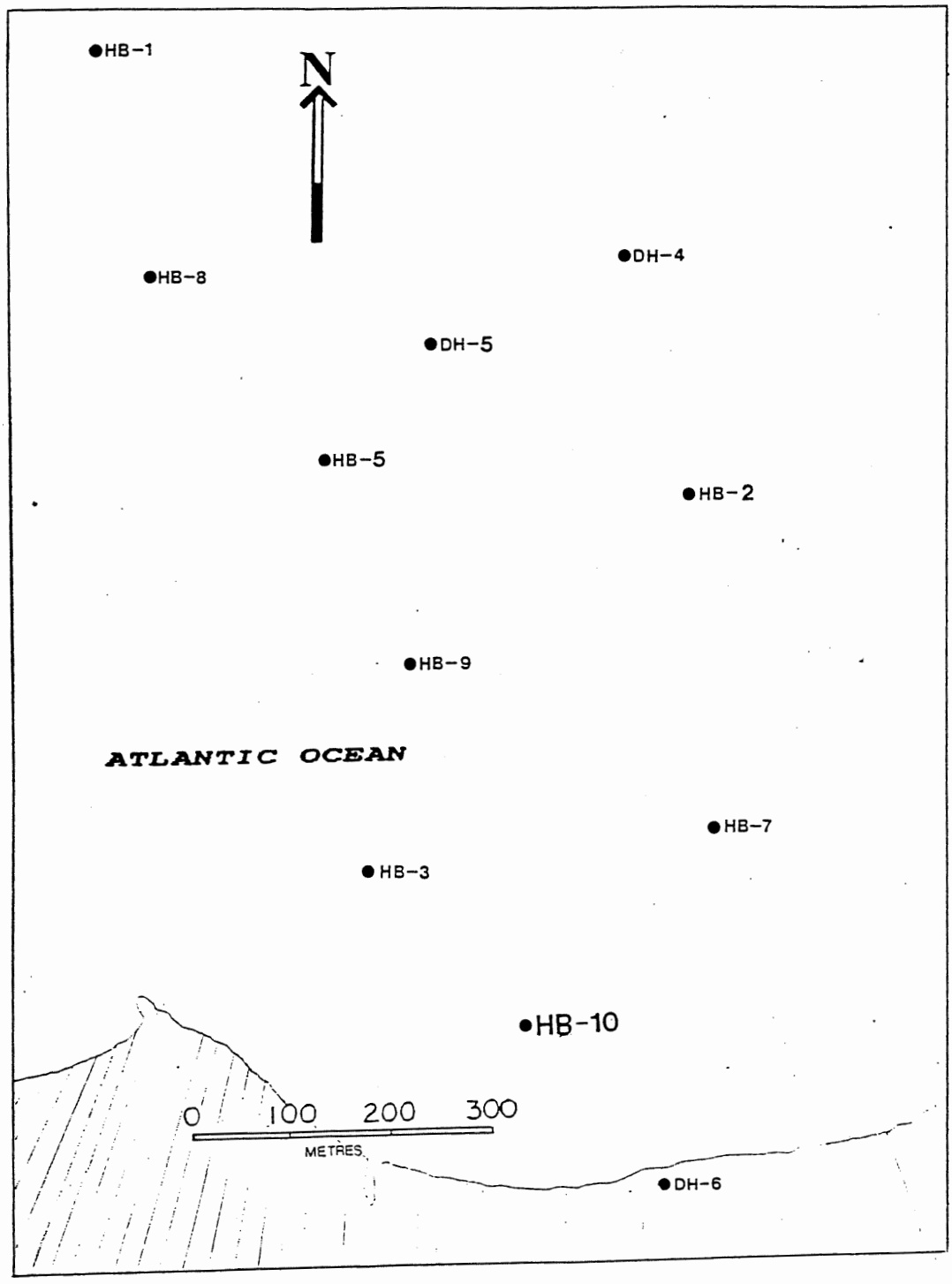

Figure 2.1 Map of the Point Aconi drill area, with labelled drill holes. This area is located on figure 1.1.

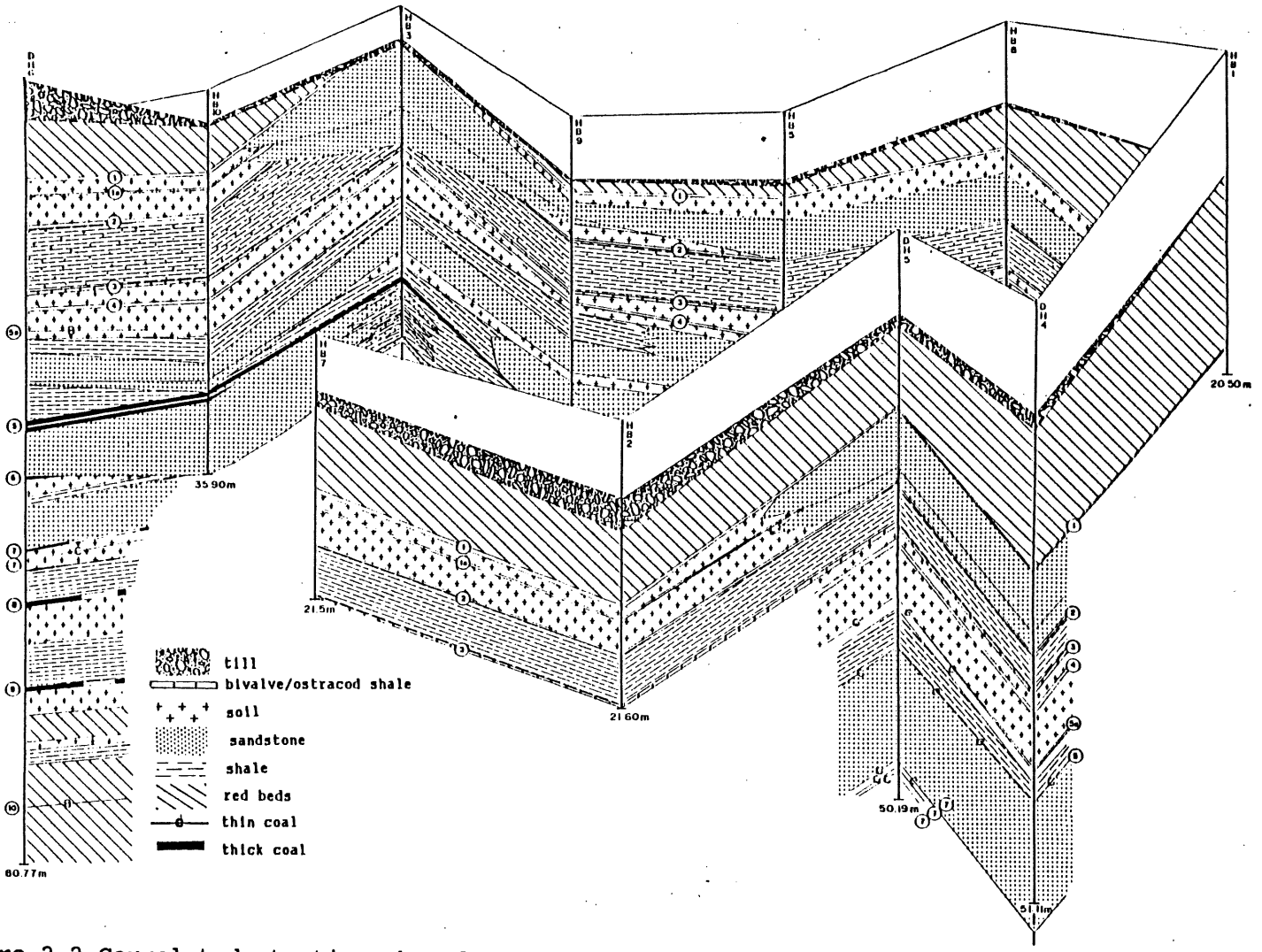

Figure 2.2 Correlated stratigraphy of the cores in Fig. 2.1 (R Naylor). The circled numbers are marker beds. Marker bed 1 = paleosol profile A, marker bed 1a is paleosol profile B, and marker bed 3 is the bivalve and ostracod-bearing shale of sample C3. The space above the till in all core logs (except DH-6) indicates depth of water.

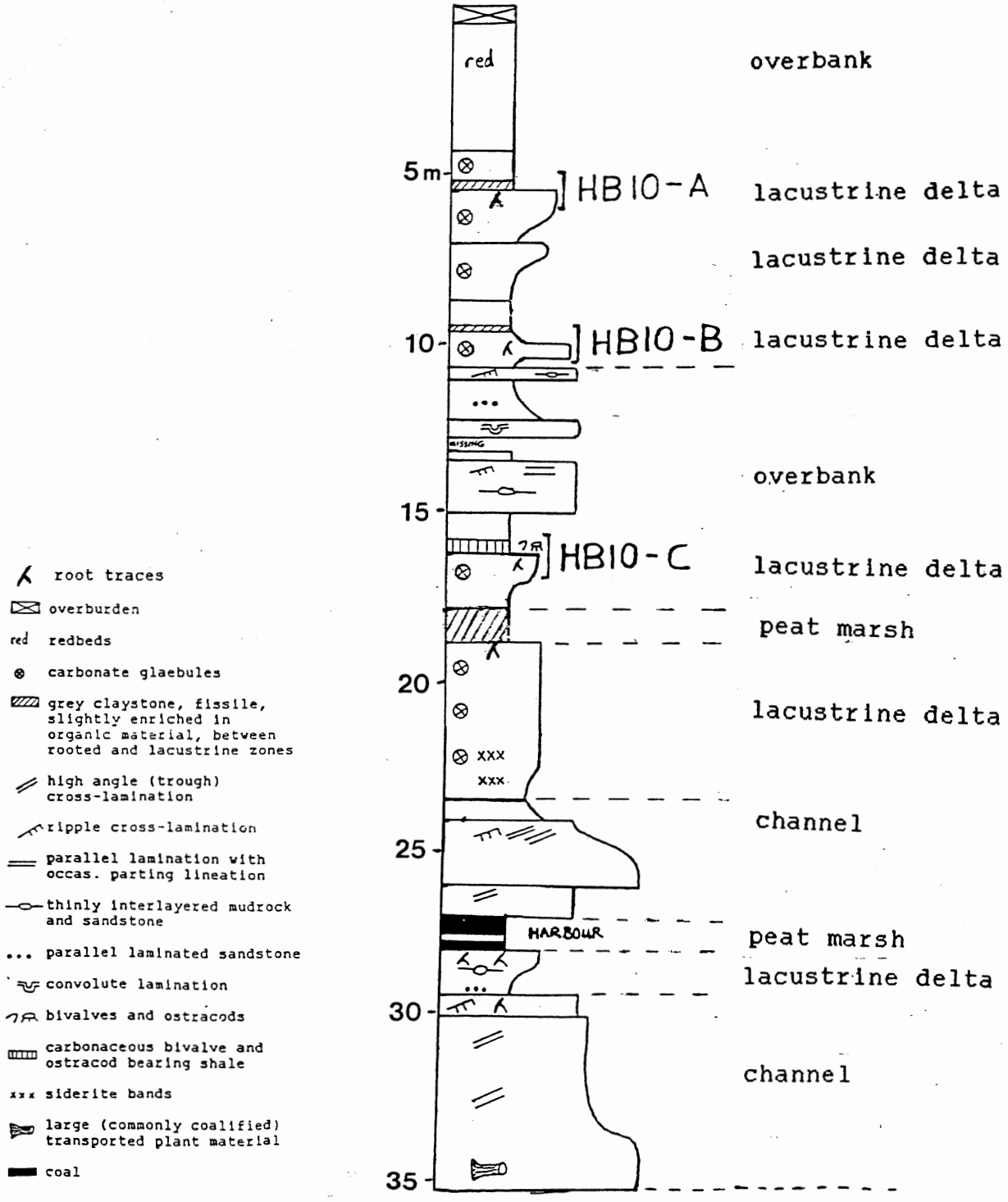

Figure 2.3 Drill log for core HB-10 with accompanying facies interpretation. Primary core log by R. Naylor. Facies interpretation based on studies of Rust et al. (1987) and Tye and Coleman (1989).

laminated sandstone. Initially, mud and fine-sand laminae were deposited possibly as muddy turbidites at the distal portion of a distributary mouth bar, followed by coarser siltstone with sand layers, and flaser, lenticular, and wavy bedding deposited as the mouth bar advanced. Overlying the siltstone is a 1 m split of the Harbour coal seam.

Above the Harbour seam is a 1 m thick siltstone layer containing sets of trough cross stratification. This siltstone may represent a minor crevasse splay deposit from a nearby channel. A sharp contact above the siltstone bed marks the base of a massive, coarse-grained sandstone, exhibiting large and small-scale cross-stratification. The sandstone fines up to a mudstone that contains some calcareous nodules and stringers. This fining upward unit, 3 m thick, is a typical channel deposit.

At approximately 23 m the mudstone begins to coarsen to a siltstone containing siderite bands, ripple cross-laminae, trough cross-stratification and common calcareous nodules. This deposit, 4 m thick, could represent a crevasse splay or lacustrine delta. At 19 m the siltstone shows a sharp contact with a friable, organic-rich claystone. At the contact the siltstone contains root traces.

At 18 m the advance of a delta into the lake resulted in a coarsening upward siltstone. This siltstone, sampled as paleosol profile C, contains numerous calcareous glaebules and root traces. Directly above profile C is a layer of carbonaceous mudstone with abundant broken shells, presumably of freshwater

bivalves and ostracods (cf. Masson and Rust 1983). The shelly layer is distinctive and laterally continuous, traceable for at least 25 km (R. Naylor, pers. comm).

The mudstone overlying profile C lessens in organic matter and has no shells. The mudstone is approximately 1 m thick, and underlies 2.7 m of alternating sandstone and mudstone beds with sharp contacts. Above this section is 0.45 m of missing core and then 0.5 m of fine sandstone with planar and convolute laminae. This type of interlayered sandstone and mudstone may represent deposition of overbank sediments.

At 12.3 m, a sharp contact separates the lower fine-sandstone from an overlying siltstone. This siltstone fines upward to a mudstone with thin, even, parallel sandstone laminae and local siderite bands, the unit possibly represents the deposit of a minor channel. At 11.1 m the mudstone has a sharp contact with a fine sandstone with mud laminae exhibiting planar, flaser, lenticular, wavy, and ripple-cross stratification, possibly indicative of an overbank deposit.

Another sharp contact separates the sandstone from 0.75 m of massive mudstone that, at 10 m, begins to coarsen to a fine sandstone. This coarsening-up (lacustrine delta) section contains paleosol profile B.

Gradually coarsening up from the B-profile is a massive silty-mudstone to siltstone that signifies the re-establishment of a delta lobe. This unit is 2.2 m thick and is massive except near the top where it exhibits ripple cross-lamination, minor

root traces, and common carbonate glaebules. From 6.6 m to 7 m in the core is a massive mudstone that coarsens upward into a fine sandstone, suggesting that deltaic sedimentation was renewed soon afterwards. The delta lobe was abandoned long enough for the incipient development of plants on the surface. Paleosol profile A developed on this delta lobe.

At the 4.25 m level the grey mudstone exhibits minor root traces and pyrite and carbonate glaebules at a contact with a 3.7 m section of massive red mudstone.

2.3 Facies Interpretation

The core is grey except for the top red mudstone (Fig. 2.2, 2.3, Plate 1). The grey rocks (including coal and organic-rich mudstones) result from deposition in a reducing environment. The sediment deposited in this facies was seasonally, if not perenially, waterlogged, resulting in the grey (reduced) colour of the strata. The red strata, however, signify a well-drained and oxidising environment (Rust et al. 1987). In the Sydney Basin, evidence suggests that a repeated cyclic rise and fall of sea level (generating cyclothems) was active during the Late Paleozoic. Ten complete cyclothems occur in the Sydney Basin, each consisting of low-stand red-beds bounded by major high-stand coal seams (Gibling 1991).

Characteristic red strata result when a drop in sea level produces a well-drained alluvial plain, incised by river channels. Later, incursion by the sea results in a peat-forming

marsh and the creation of the thick coal seams of the Sydney Basin. Based on palynological data, the estimated duration of each cyclothem is 200-300 ka. The coal-bearing strata underlie much of the Gulf of St. Lawrence, implying that the cyclothems may have covered an area of more than 80,000 km^2.

The regional sea-level changes reflect the combined influence of tectonics, subsidence, and sediment supply, however the repetitious regularity of the cycles suggests glacial eustacy may have been the dominant factor (Gibling 1991).

2.4 Summary

In general, core HB-10 fines upward from channel sandstones at the base to delta siltstones and overbank mudstones near the top. The paleosols formed on coarsening upward sediments, likely lacustrine deltaic deposits that became subaerial, albeit briefly. The lacustrine delta facies was an unstable one, with rapid subsidence and renewed sedimentation causing quick burial of the three profiles.

CHAPTER 3 PROFILE DESCRIPTIONS

3.1 Introduction

This chapter describes the three paleosol profiles in detail, combining the macroscopic observations from the core log and hand samples with the microscopic observations from thin sections. See Appendix B for a glossary of soil terminology.

3.2 Profile Descriptions

The profile descriptions are from the core log, hand sample, and petrographic observations. Each profile is divided into sections of similar characteristics, starting at the top of each profile with Unit 1 (Fig. 3.1).

In all samples, except B3, matrix clays comprise the main grain type with matrix-supported fabrics (Table 3.1). Quartz is the second most common grain type in fourteen samples, and most quartz grains appear sub-rounded according to the classification of Powers (1953). Although the samples contained corroded plagioclase, the proportion of feldspar grains was relatively uniform down through the profiles. The apparent scarcity of feldspar in these samples is probably a result of a feldspar-poor parent material rather than weathering. Marshall (1977) showed that feldspar is an easily weathered mineral which should decompose quickly in paleosols. If destruction of the grains had occurred in the weathering environment, there should be an increase in the number of grains away from the surface where

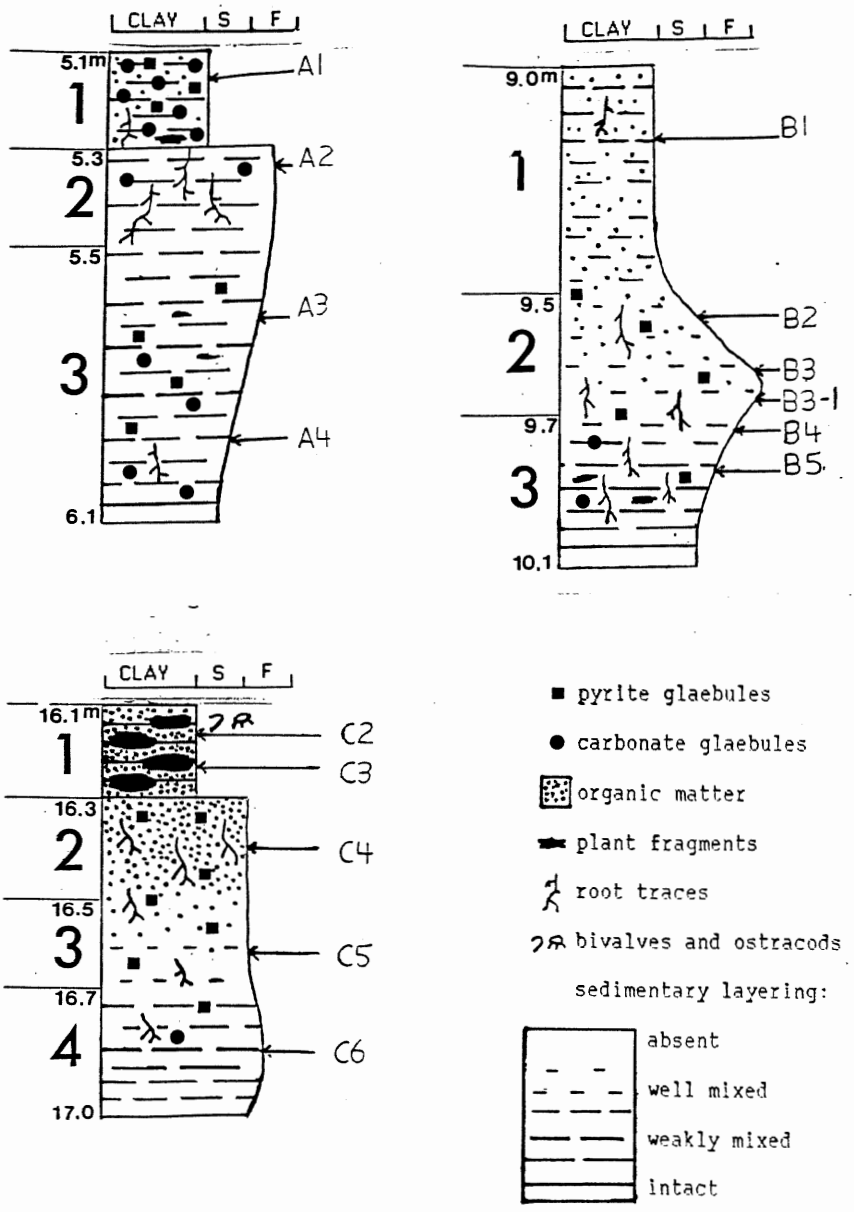

Figure 3.1 Grain sizes and pedogenic features of the three sampled paleosol profiles with unit divisions indicated. Clay = claystone, S = siltstone, F = fine sandstone.

	Quartz+Feldspar	Mica	Glaebules	Matrix	Shells
A1			23	77	
A2	9		20	71	
A3	11	4	2	83	
A4	32	13	5	50	
B1				100	
B2	20	3	3	74	
B3	51	7	1	41	
B3-1	41	10		49	
B4	29	7	1	63	
B5	1	-	29	70	
C2	10			60	30
C3	5			90	5
C4	1			99	
C5	1		4	95	
C6	16	10	3	71	

Table 3.1 Modal compositions of the fifteen samples expressed as the percentage of 200 point counts on thin sections. The category "shells" refers to bivalves and ostracods. Matrix represents grains less than 30 microns in diameter. Because of the difficulty in distinguishing silt-sized quartz from silt-sized potassic feldspar in thin section, quartz and feldspar are grouped in the same category.

weathering is most intense (Leckie et al. 1989).

Glaebules occur in thirteen of the paleosol samples. Various combinations of carbonate minerals, pyrite, and chert occur as nodules and concretions.

Samples B2 and C4 exhibit the highest degree of sediment mixing, with sedimentary layering obliterated in these samples. However, relict sedimentary layering exists in most samples, a characteristic of immature hydromorphic soils. (Soils need to be well-drained at least periodically before significant leaching and horizon development can occur (Buringh 1970).)

Profile A

Profile A is 1 metre long and shows many features of pedogenesis, including root traces, organic matter, and abundant carbonate glaebules. However, the well preserved sedimentary layers betray the pedogenic immaturity of this profile, with only incipient horizons developed.

Unit 1, 5.1 m to 5.3 m, sample A1 Unit 1 is a medium-dark grey claystone with minor root traces and abundant organic matter. Approximately 25% of the grains in this section are calcite and pyrite glaebules. The glaebules are all less than 1 mm in diameter, including an elongate and tapered patch of carbonate nodules possibly occurring in replacement of a former root (Fig. 3.2a).

Unit 2, 5.3 m to 5.5 m, sample A2 Unit 2 is a mottled, light-grey/brown argillaceous sandstone with carbonate nodules

and root traces. The fossil roots are small (up to 2 mm thickness), branched and tapered, and filled with a light-brown carbonate (effervesces slightly with HCl).

Unit 3, 5.5 m to 6.1 m, samples A3 and A4 This basal unit is a bluish-grey sandy siltstone containing carbonate and pyrite glaebules (up to 1 cm diameter) and minor root traces and plant fragments. Some of the carbonate concretions exhibit a fine-crystalline rind and a coarser centre (Fig. 3.2b), possibly reflecting crystallization around decaying plant matter (Berner 1981). Near the top of Unit 3, the sedimentary layering is slightly more mixed than at the base of the profile (Fig.3.3a).

Profile B

This profile is 1.1 m long and shows weak pedogenic development.

Unit 1, 9.0 m to 9.5 m, sample B1 The top 50 cm of the profile is a medium-grey, fissile mudstone with partially mixed sedimentary layering (Fig. 3.4a), and variable amounts of plant fragments and other organic matter, including one large (5 cm) plant fossil imprint.

Unit 2, 9.5 m to 9.7, samples B2, B3, B3-1 This unit is a light-grey, fine-grained argillaceous sandstone at the base (B3-1, B3), which fines up to a siltstone (B2). Sample B3 contains a silt-filled krotovina (Figure 3.4b), presumably material from the overlying siltstone of sample B2. Calcite cement occurs between quartz grains in part of thin section B3.

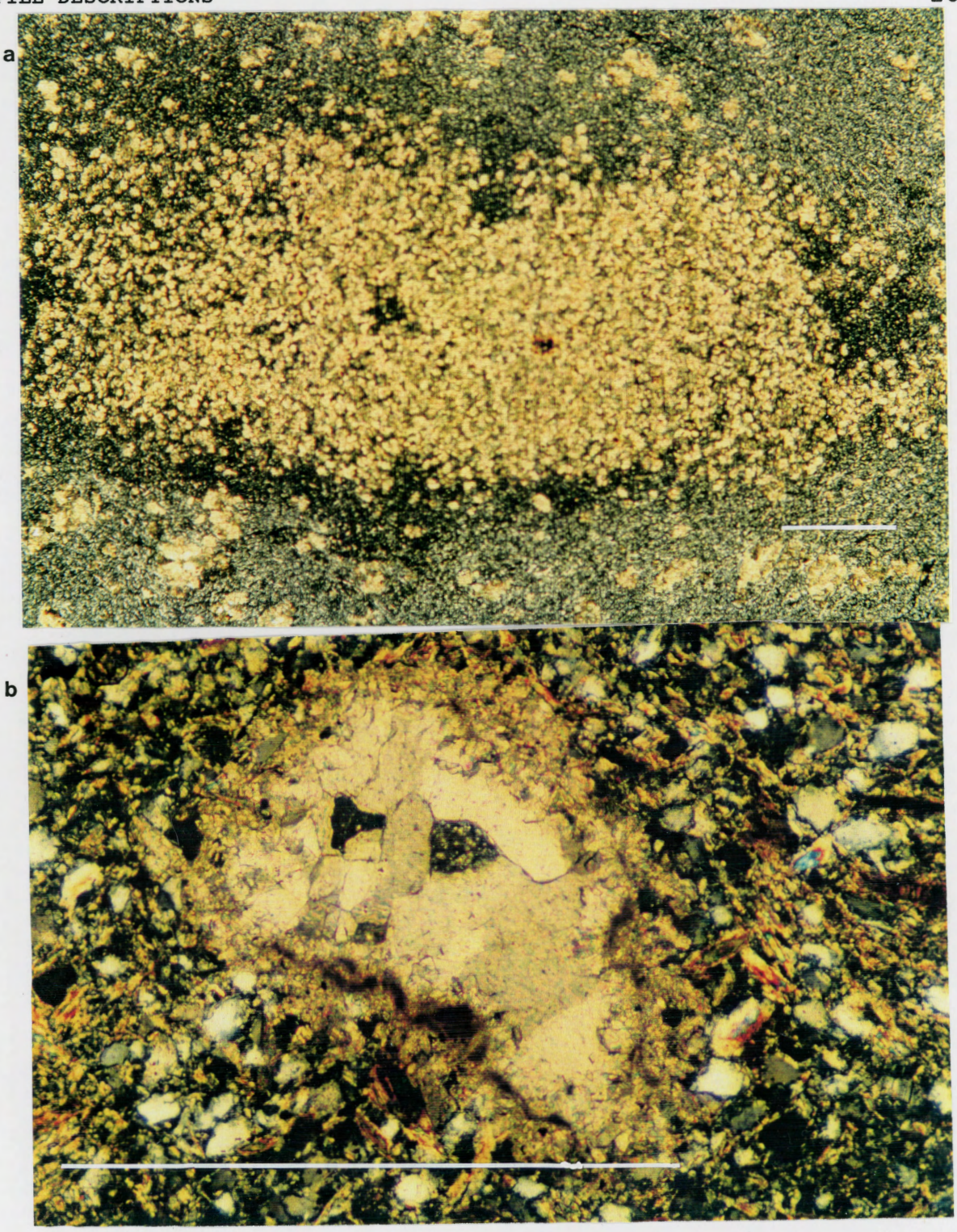

Figure 3.2 a) Sample HB10-A1. Carbonate glaebule patch possibly formed in replacment of a former root or other organic matter (xn). Scale bar = 1 mm. b) Sample HB10-A3. Carbonate concretion with a relatively coarse-grained centre and a finer grained rim, which may indicate different growth phases of carbonate around a decomposing root (xn). Scale bar = 1 mm.

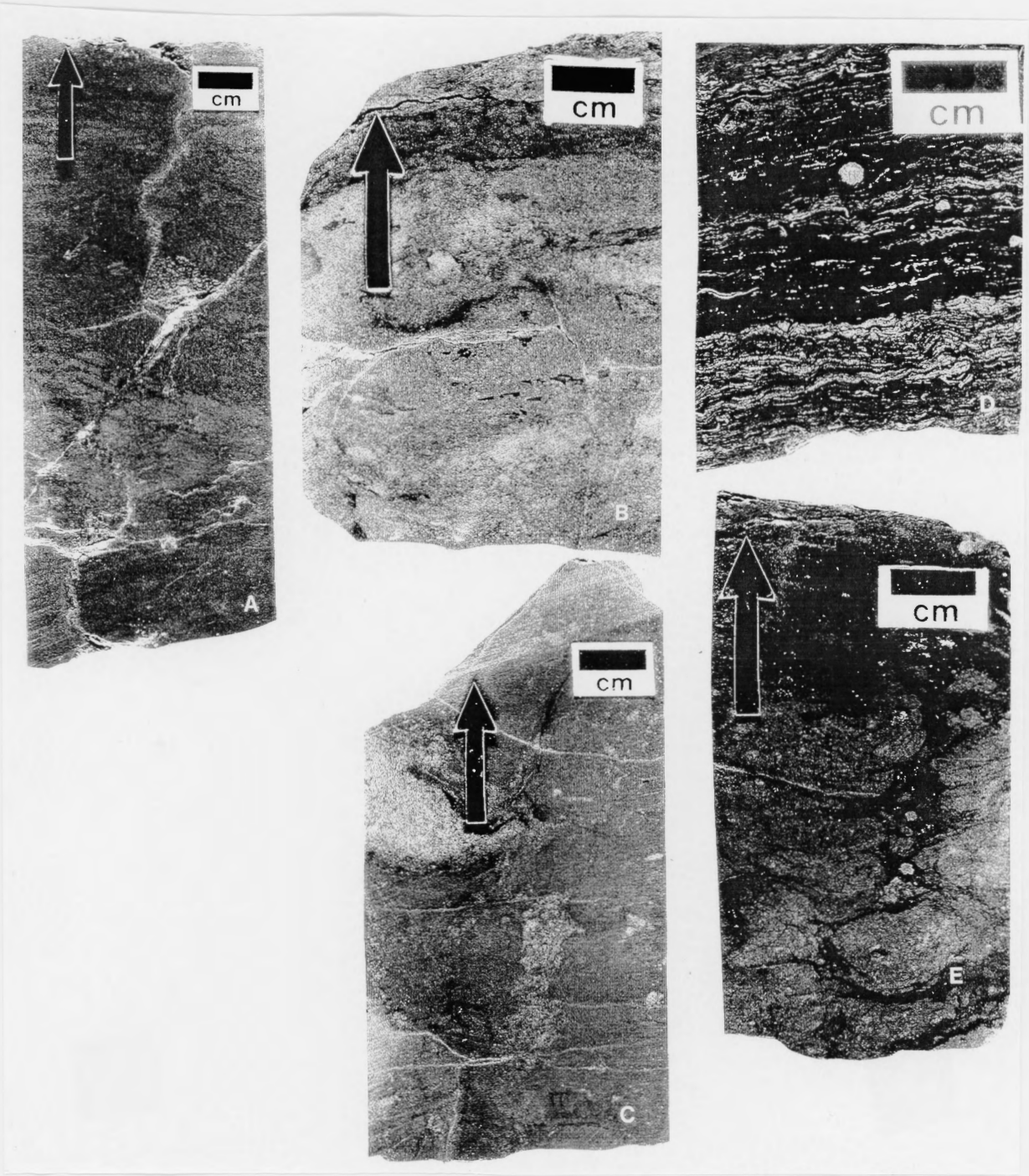

Figure 3.3 Pedogenic features of hand samples. a) Sample HB10-A3. Pale grey/dark grey mottling and carbonate patches in a medium grey siltstone. b) Sample HB10-B2. Siltstone with mottled grey colour. Black streaks are fine grained organic matter. c) Sample HB10-B4. Large (ca. 3cm) white patches are fine sand krotovinas in siltstone. d) Sample HB10-C2. White shells define layering in an organic-rich shale. e) Sample HB10-C4. Photo shows mottled colour and streaked organic matter. Arrows point in a younging direction.

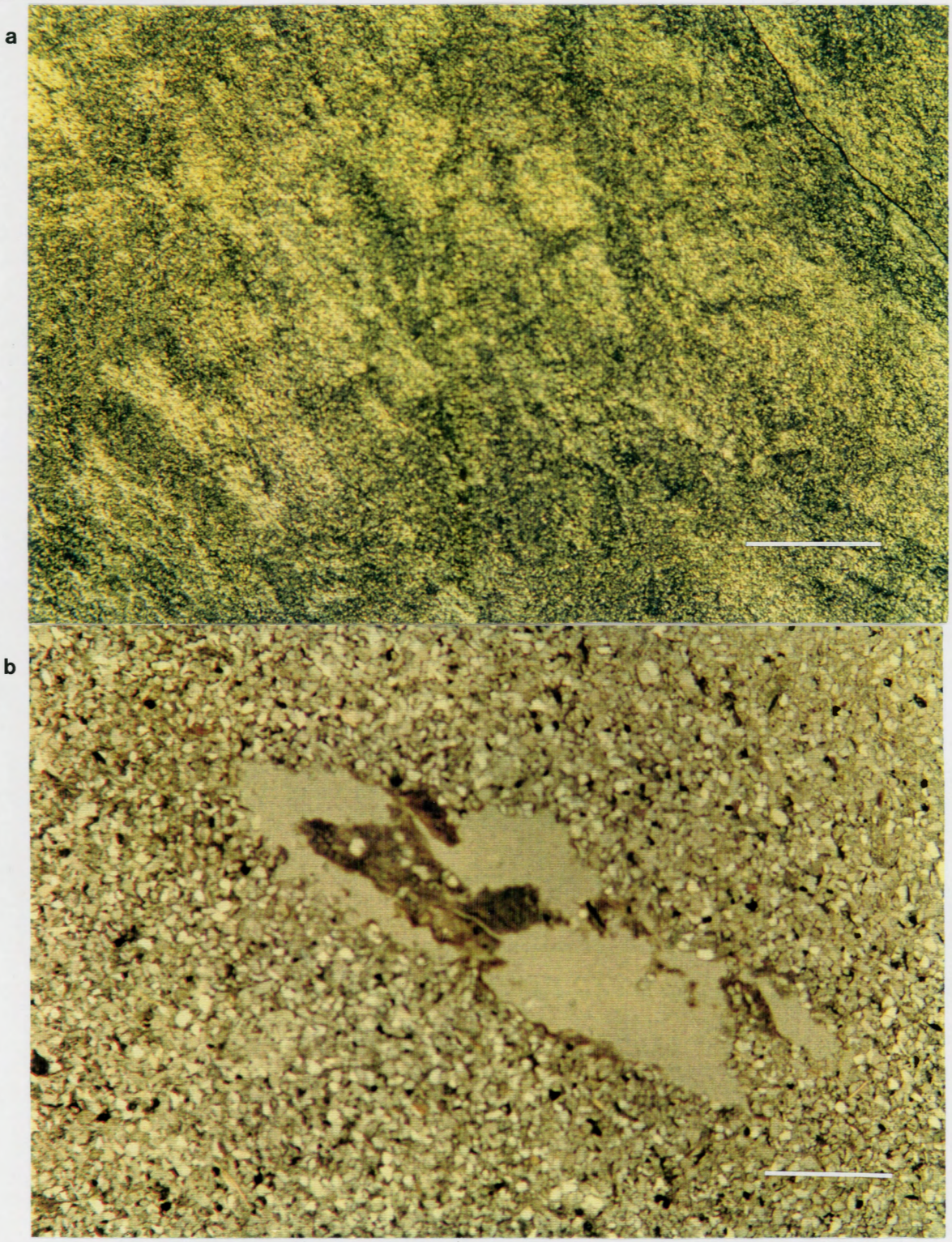

Figure 3.4 a) Haploidization in sample HB10-B1. An example of insepic plasmic fabric (xn). b) Sample HB10-B3. Krotovina remnant. The dark fine grained material in the void centre is the krotovina (the rest was removed in thin section processing). The silt sized material in the krotovina corresponds to the silt-sized overlying sediment. Scale bar = 1 mm in both photos.

Sample B2 is a medium-grey fissile siltstone with mottled colouring, and root traces (Fig. 3.3b). The root traces exhibit typical tapering, contain much organic material, and are surrounded by an organic-free argillan of very fine-grained material. Outside of the root traces, sample B2 has skelsepic fabric with no visible sedimentary layering, and clustered concentrations of organic material.

Unit 3, 9.7 m to 10.1 m, samples B4, B5 The bottom 40 cm of profile B is a moderately fissile, medium to dark grey (mottled) siltstone which coarsens up to sandy-siltstone. It contains root traces, plant fragments, carbonate glaebules and disseminated pyrite, with rare 1 cm pyrite nodules. Sample B4 has 1-4 cm long root traces containing fine-sand krotovinas (fine sand that washed down from the overlying argillaceous sandstone) in a siltstone matrix (Figs. 3.3c, 3.5). In addition to the krotovinas, sample B4 shows minor pyrite and carbonate concretions and argillasepic fabric.

In thin section, sample B5 exhibits root traces filled with pyrite, carbonate, and chert concretions (Figures 3.6, 3.7). Despite abundant root traces, sedimentary layering is weakly mixed in sample B5.

Profile C

Unit 1, 16.1 m to 16.3 m, samples C2, C3 The top of profile C is an organic-rich mudstone. At 16.2 m is abundant, though mostly broken, shelly material (0.5 mm to 3 mm diameter) of

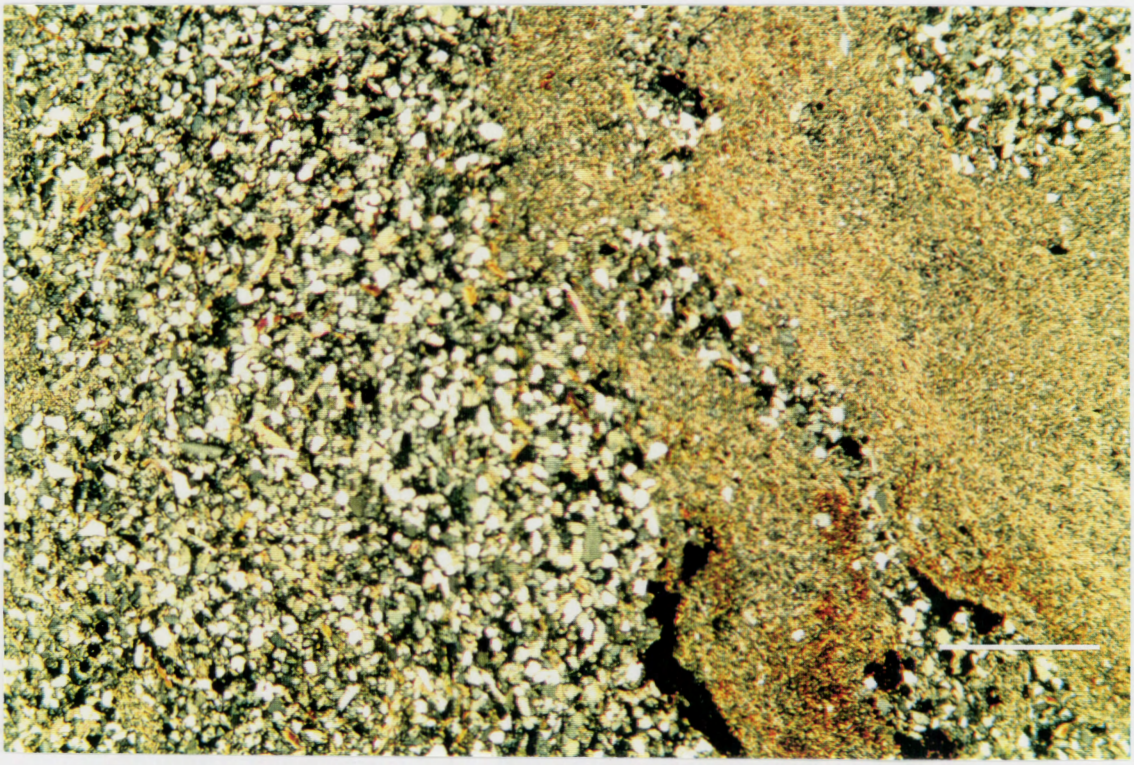

Figure 3.5 Sample HB10-B4. Sand krotovina in silt matrix. The fine sand comes from the overlying wackestone (xn). Scale bar = 1 mm.

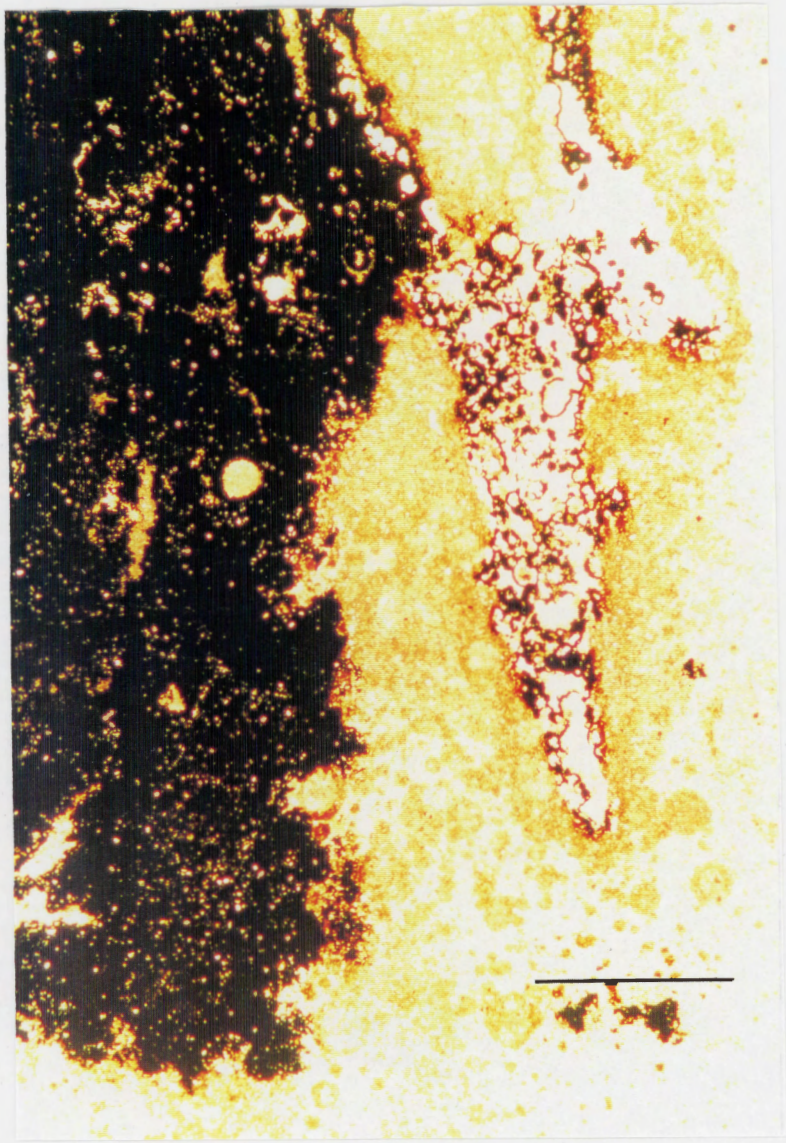

Figure 3.6 Sample HB10-B5. Elongate root trace, beside (black) pyrite concretion. Note the tapered shape of the root trace which contains pyrite and carbonate (ppl). Scale bar = 1 mm.

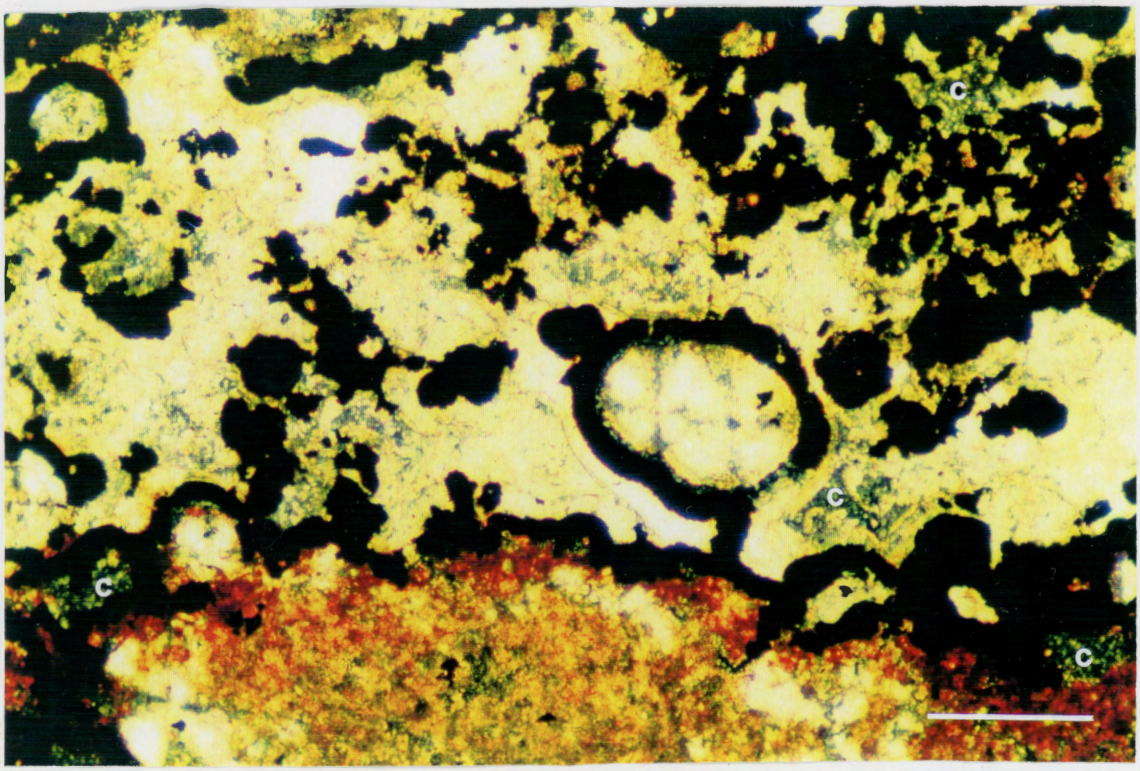

Figure 3.7 Sample HB10-B5. Detail of the elongate root trace of Figure 3.6. Bright white grains are carbonate, also pyrite (black patches) and chert (c) (xn). Scale bar = 0.1 mm.

ostracods and possibly other fresh-water fauna (Figs. 3.3d, 3.8a,b) (cf. Masson and Rust 1983). Figure 3.8b shows one unbroken ostracod, possibly an example of Carbonita (Masson and Rust 1983). Figure 3.10a is a photomicrograph of the organic-rich mudstone of sample C3.

Unit 2, 16.3 m to 16.5 m, sample C4 Next in the profile is a dark grey siltstone that is fissile, has mottled colouring, abundant root traces, chert and pyrite patches, and contains much organic matter (Fig. 3.3e, 3.9b) giving the rock a distinct hydrocarbon odour. All sedimentary layering is obliterated in this unit, with the sediment mixing resulting in an argillasepic fabric.

Unit 3, 16.5 m to 16.7 m, sample C5 A medium-grey siltstone, containing a 5 cm-thick bedding-parallel layer dense with carbonate glaebules that coalesce to form a fragile "crumbly" structure. Thin-section C5 contains two carbonate/pyrite/chert concretions, with pyrite and chert possibly replacing the carbonate (Figures 3.10a,b).

Unit 4, 16.7 m to 17 m, sample C6 The base of Profile C is a medium-dark grey sandy-siltstone, showing minor pedogenic features of a few pyrite and carbonate glaebules, rare root traces, and minor sediment mixing.

3.3 Summary

Profile A is the least developed paleosol. Profile B is weakly developed, and profile C shows the strongest pedogenesis and is

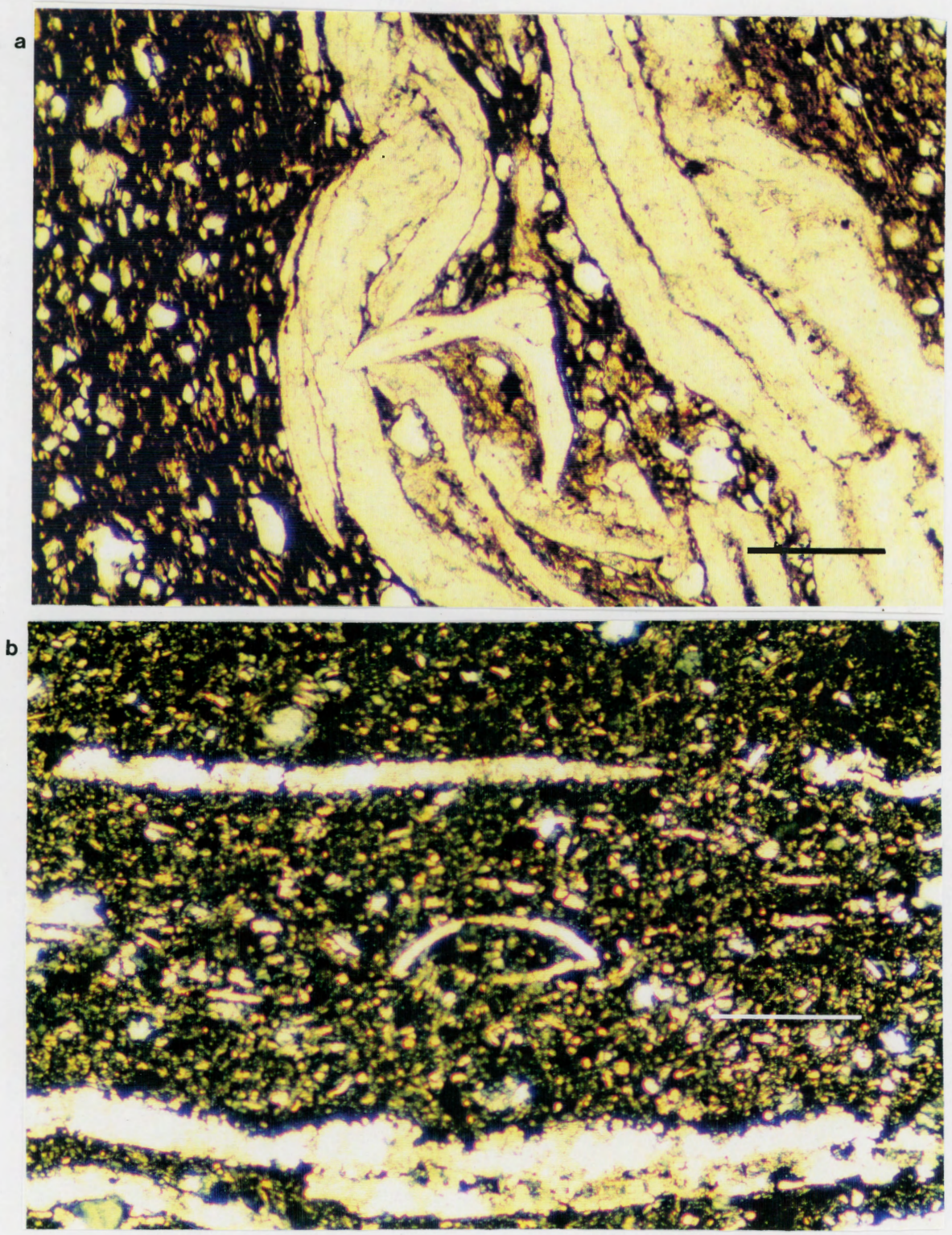

Figure 3.8 a) Sample HB10-C2. Boomerang-shaped object is a fish vertebra between compressed bivalve(?) shells, in black shale (ppl). b) Sample HB10-C2. Ostracod with unidentified shell fragments (xn). Scale bar = 0.1 mm in both photos.

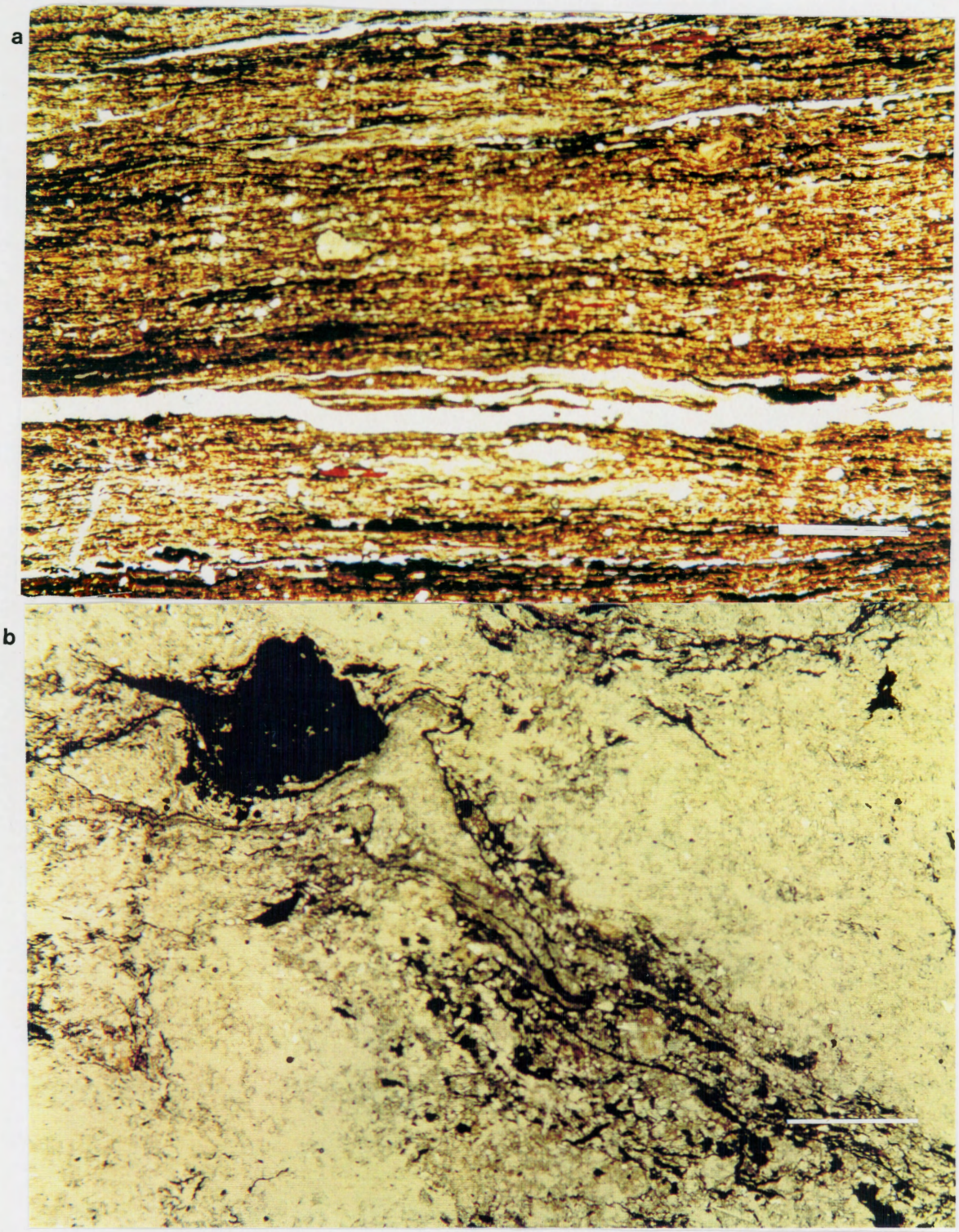

Figure 3.9 a) Sample HB10-C3. Organic-rich shale. Elongate void occurred when thin-section preparation removed a section of coal. Quartz and impure organic material predominate in the rest of the slide (xn). b) Sample HB10-C4. Root traces (?). Large black spot is pyrite, black streaks are organic material with tapered traces (ppl). Scale bar = 1 mm in both photos.

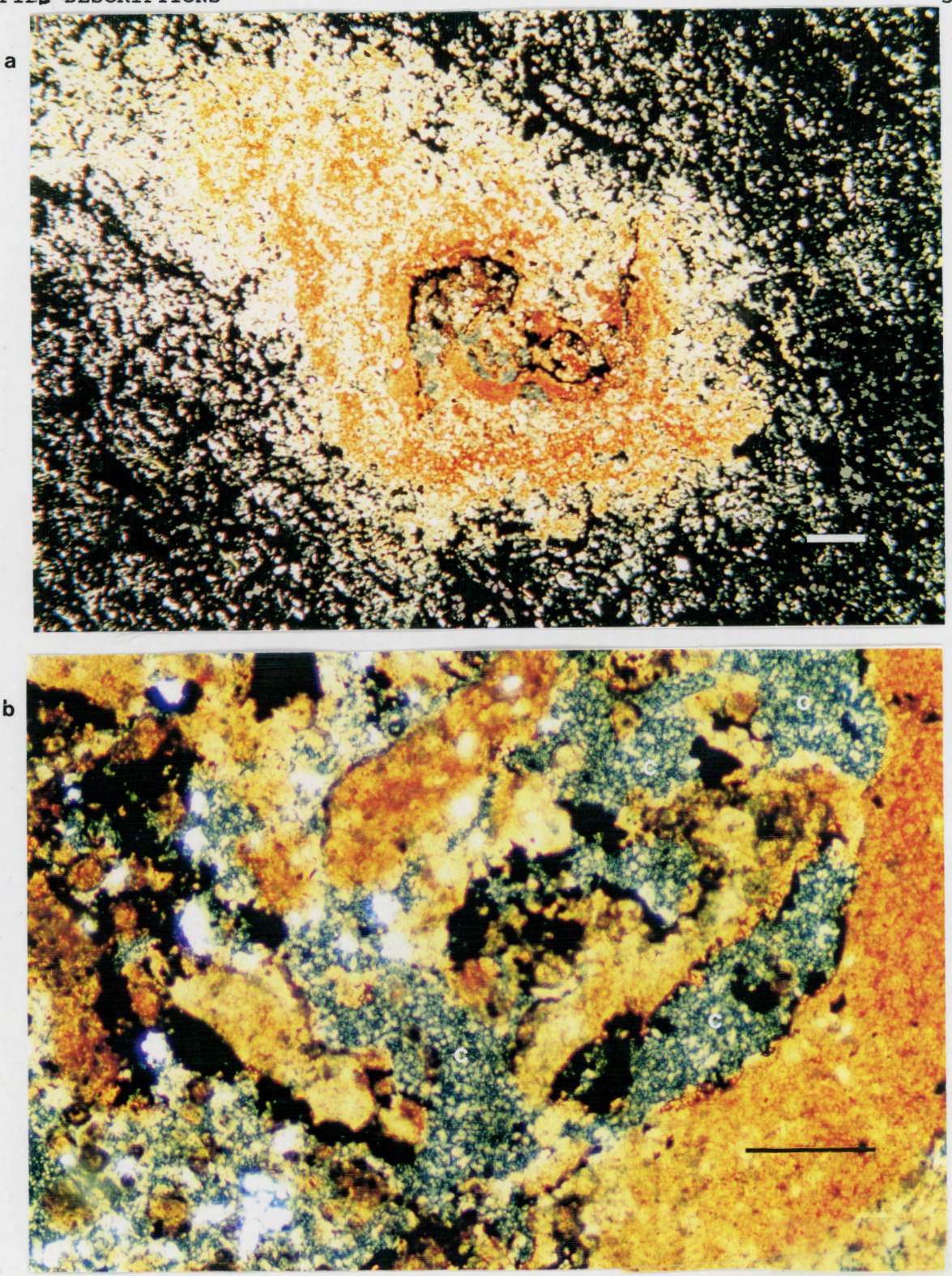

Figure 3.10 a) Sample HB10-C5. Diffuse spots are carbonate glaebules (xn). Scale bar = 1mm. b) Sample HB10-C5. Detail of the concretion in Figure 3.10a. (Light brown and white=carbonate patches, black=pyrite, and chert (c)(xn). Scale bar = 0.1 mm.

moderately developed (refer to Appendix C for definitions of paleosol development). Although the roots are abundant in profile A, sedimentary layering is only slightly disturbed, indicating that the soil was host to the plants for a relatively short time. Profile B appears to have originated on a lacustrine delta, but plant growth continued after the delta was abandoned and sedimentation occurred as overbank mud deposits. Consequently, profile B does not have a clearly defined top.

The immaturity of profiles A and B probably reflects an increased rate of sedimentation in contrast to profile C.

Although all three profiles are grey and therefore reduced, the profiles progressively lessen in organic matter and plant fragments from the stratigraphically lowest (profile C) to the highest (profile A), possibly suggesting that a gradual fall in relative sea level improved drainage conditions for the higher strata in the core.

3.4 Discussion and Conclusions

Tye and Coleman (1989) analyzed lacustrine deltas in the Atchafalaya Basin of the Mississippi Delta. The following is a comparison of the Carboniferous Sydney Basin to the modern Mississippi Delta.

The lacustrine delta environments were unstable, with rapidly changing surface features. One Atachafalaya delta, the Lake Fausse Pointe delta, prograded 6.5 km, partially filled the lake, and covered an area of over 29 km^2 in twelve years. When

the delta was abandoned, soils developed on the delta surface. However, subsidence soon resulted in the drowning of the soil and the development of a peat-marsh.

Paleosol profile C formed under similar conditions as the delta soils described by Tye and Coleman (1989). The profile developed on an abandoned delta lobe, but the paleosol was not well developed before it was drowned by subsidence. The carbonaceous shale of samples C2 and C3 formed on top of profile C in the resulting peat marsh. That the carbonaceous mudstones are laterally traceable for a distance of at least 25 km (R. Naylor 1992 pers. comm) implies that an extensive drowning of the delta plain occurred. Such extensive flooding suggests the cut-off of a major supply of sediment, possibly by the avulsion of a major delta feeder channel.

Above the carbonaceous shale layer, the presence of mudstone indicates renewed detrital input. In the Sydney Mines area, 15 km away from the Point Aconi drilling site, fluvial channel deposits above the organic mudstone layer indicate that a drop in base level permitted the incision of the channels (R. Naylor 1992 pers. comm).

Profile B formed in an environment of more or less continuous deposition. The lack of a well-defined top or bottom to profile B indicates that sedimentation kept pace with plant development. Profile A has a sharply defined top, however the limited sediment mixing in this profile suggests that the delta lobe was not inhabited by plants for long before being drowned.

Lowered base-level resulted in the red-bed deposits at the top of core HB-10. Like the Harbour coal seam and the shelly organic mudstone, the red-beds extend for at least 25 km in correlated strata (R. Naylor 1992 pers. comm) indicating the base level fluctuations were major events.

The paleosols probably developed quickly on the unconsolidated deltaic sediments, but subsidence resulted in the rapid burial of the soils.

CHAPTER 4 PALEOSOL GEOCHEMISTRY

4.1 Introduction

This chapter addresses the microscale observations of the samples. These include data obtained from the electron microprobe (EMP), the scanning electron microscope (SEM), and x-ray fluorescence (XRF).

4.2 Mineral Chemistry

Petrographic observations revealed a concentric banding of minerals in many glaebules. Electron microprobe analysis of the mineral compositions enabled the determination of the composition of the concretions, and helped to establish the conditions under which pedogenesis took place.

EMP analysis of the concretions in the samples shows that the concretionary rings are 2-20 μm thick, and that all analysed concretions contain at least two different mineral phases (Figs. 4.1a,b). Mineral identifications were based on: qualitative petrographic observations, electron backscattering, (which is directly proportional to average atomic number), and quantitative EMP analysis.

Table 4.1 contains the chemical analyses and corresponding mineral names of some of the concretions. The concretions consist of pyrite, chert (identified in thin section), and carbonate minerals (calcite, siderite, and kutnahorite). Carbonate nomenclature follows Dana and Dana (1952) and Berry et al.

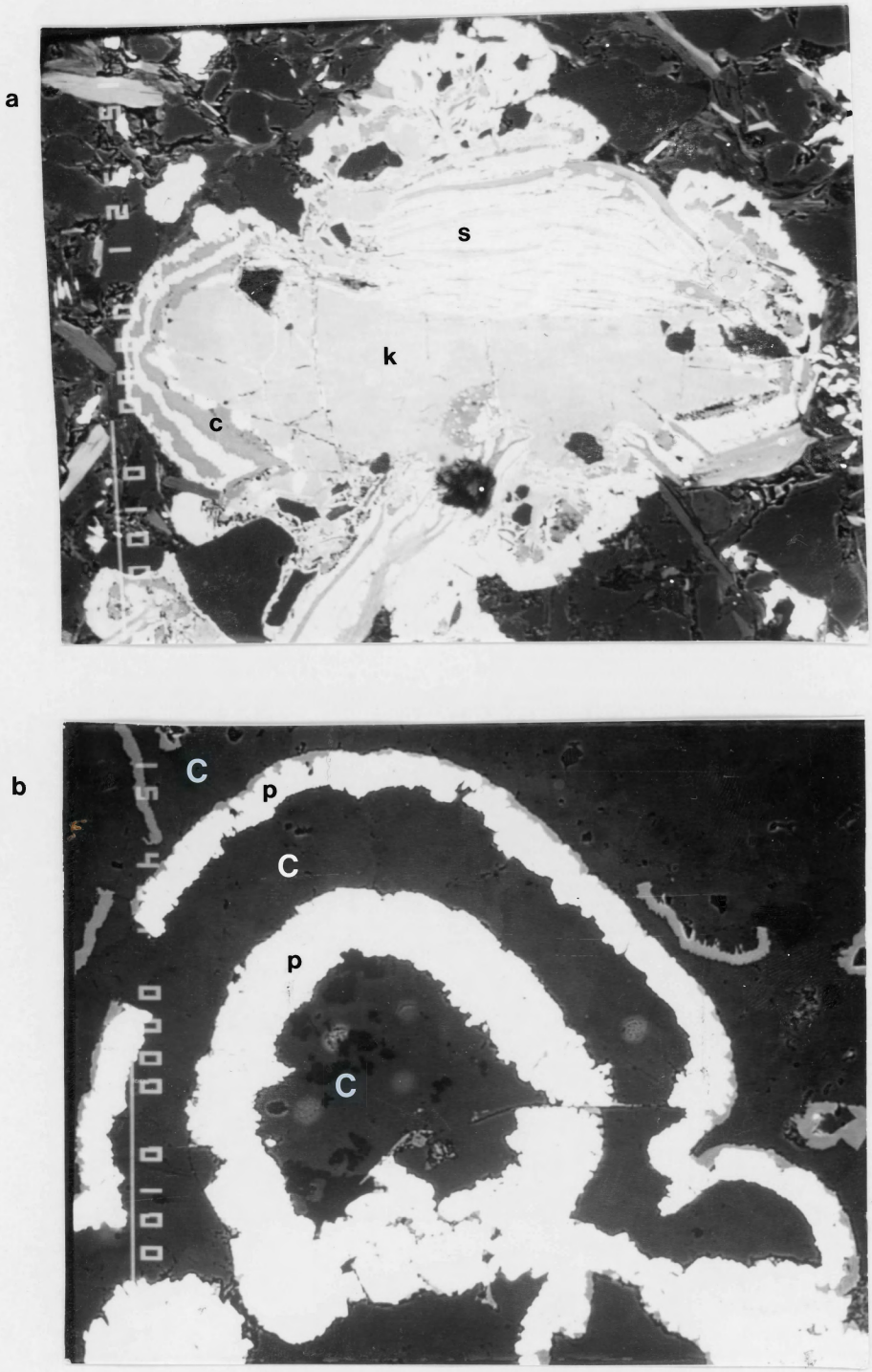

Figure 4.1 a) Sample HB10-C6. Backscattered electron micrograph of carbonate concretion, with a complex interlayering of calcite (c), kutnahorite (k), and siderite (s). b) Sample HB10-B5. Electron micrograph of calcite and pyrite concretion. Note the rough outer edges of calcite (c),and the more even outer edge of pyrite (p) where acidic deposition of pyrite resulted in the partial corrosion of calcite. Scale bar (white line) represents 100 microns.(1983).

	FeO	MnO	MgO	SrO	TiO_2	CaO	Mineral	
A1	0.00	0.00	0.47	0.01	0.00	52.54	calcite
A1	35.55	1.68	4.59	0.04	0.10	4.38	siderite
A4a	43.75	3.88	2.98	0.00	-	9.06	siderite
A4b	1.63	5.53	0.18	0.00	-	58.48	calcite
A4	50.16	2.59	3.42	0.04	-	5.19	siderite
A4	45.86	2.71	3.35	0.00	-	7.16	siderite
B5a	43.85	0.16	0.09	0.10	0.10	0.40	pyrite
B5b	1.14	1.97	0.24	0.06	0.00	41.64	calcite
B5c	1.38	2.61	0.22	0.04	0.00	53.75	calcite
C2	0.01	0.00	0.30	0.23	0.00	56.30	calcite
C2	0.84	0.83	0.25	0.10	0.00	53.98	calcite
C5a	0.53	15.60	0.67	0.06	0.01	36.31	Mn-calcite
C5b	5.74	3.13	0.57	0.07	0.00	41.81	calcite
C6a	33.19	9.22	2.59	0.03	0.15	6.30	siderite
C6b	0.88	25.56	1.00	0.02	0.02	27.65	kutnahorite
C6c	4.64	5.89	1.30	0.05	0.00	49.30	calcite
C6	0.06	22.10	0.74	0.05	0.00	29.38	Mn-calcite

Table 4.1 Electron microprobe chemical analyses of eleven concretions. Letters a,b,c beside the sample numbers indicate the scanning of different layers within the same concretion. A dash (—) shows where an element was not determined. Analyses are in oxide weight percent.

Ideally, calcite has a complete solid solution with Mn to rhodochrosite, however for MnO/CaO ratios greater than 0.8 the more stable phase is kutnahorite. As a result, probe point C6b is labelled as kutnahorite, and C5a and C6 are labelled Mn-calcite. Calcite has a partial substitution with Fe toward siderite up to 13.05% FeO. Mg substitutes to 7.28% MgO, above which dolomite forms. Siderite has a complete solid solution to rhodochrosite and magnesite, and can accommodate up to 12% CaO. Rhodochrosite can have up to 13% MgO and a complete series to calcite, although highly calcian material is rare.

4.3 Discussion of Mineral Compositions

The cations of these minerals - iron, calcium, manganese, and silica - are released by the weathering of detrital grains such as feldspars, micas, and clays (Foth 1984), or they can be transported to the site of authigenesis in solution (Wilkinson 1989). However, fresh-water lacustrine environments often lack significant sulphide and carbonate ions. There are four potential sources of carbonate and sulphur: (i) erosion of the Early Carboniferous Windsor Group evaporites could lead to input of sulphate and carbonate as detritus in the Morien Group (Rust et al. 1987); (ii) plants absorb and concentrate airborne sulphur through their leaves, and the subsequent death of the plant releases sulphite in the soil (Foth 1984); (iii) carbonate ions form when ammonia and carbon dioxide (liberated by the bacterial decomposition of organic matter) combine in water (Berner 1981);

and (iv) the infuence of marine waters could bring sulphur and carbonate ions into the soils.

The concretionary banding of alternating mineral phases suggests a complex growth history. The pyrite and carbonate concretion of sample B5 (Fig. 4.1b) may represent pH fluctuations in soil water. The carbonate ion solubility strongly depends on pH. In soils of pH <7.8, calcite will not precipitate, however low pH favours pyrite deposition (Retallack 1990). Sehgal and Stoops (1972) found that concretionary carbonate formed during dry alkaline periods, but during a wet season high acidity caused the carbonate to be partially corroded and replaced by ferruginous material. Krumbein and Garrels (1952) recognized that fluctuations in pH can also result from a periodic buildup and then degassing of CO_2 as a result of bacterial respiration. As well, concretions containing chert pyrite and carbonate may result from acidic fluids in the soil reacting with iron silicates and converting them to pyrite and chert, corroding carbonate in the process (Krumbein and Garrels 1952).

The dense, bedding-parallel layer of carbonate concretions in sample C5 formed as a result of solute diffusion into the sediment from the overlying lake water, precipitating at a pH front created by bacterial respiration. An unlimited (or replenished) source of solute would be required to create such a dense packing of carbonate concretions (Krumbein and Garrels 1952; Wilkinson 1989).

Concretions such as those in samples A1, A4, C5, and C6

(Table 4.1) contain a combination of the carbonate minerals calcite, siderite, and manganocalcite (kutnahorite). Barnaby and Rimstidt (1989) noted that the Fe/Mn ratio of carbonate minerals increases with increasing Eh of the solution. Because Fe and Mn have different oxidation potentials, an increase in Eh can result in the oxidation of Fe from 2^+ to 3^+, while Mn remains at 2^+. The carbonate anion can accommodate only those cations with a charge of 2^+ and thus, the cation content of carbonate minerals is in part a reflection of Eh conditions. However, the oxidation and reduction of calcium and carbonate ions require extremes of Eh that surpass most soil environments, therefore the model of Barnaby and Rimstidt (1989) cannot explain the overgrowths of calcite with siderite and kutnahorite. An alternative explanation by Wilkinson (1989) favours ion diffusion as the limiting factor. The ion diffusion model assumes there is an excess of carbonate anions, but limits the number of cations (Ca, Fe, and Mn). When the concentration of one cation becomes sufficiently low, the precipitation of another begins, creating the multi-mineralic layering of the carbonate concretions.

In summary:

1) Concretions with alternating pyrite and carbonate ($\pm$chert) layers probably result from fluctuations in ground water pH, a possible result of bacterial respiration.

2) Concretions containing alternating carbonate minerals likely result from limited cations in diffusive transport.

3) Carbonate and sulphate ions are present in ground water solution, and liberated by bacterial decomposition of organic matter.

4) Many, if not all, concretions formed prior to deep burial, as shown in the bedding perpendicular layer of concretions in sample C5, and the concretionary root fill of sample B5.

4.4 Scanning Electron Microscope

Four samples (A1, A2, B2, and B3) were selected for analysis on a scanning electron microscope. These samples had been scanned for potential silica overgrowths.

Identification of minerals is made using the EDS (energy dispersive spectrometer) which provides a chemical analysis at selected visual positions and backscattered electron imaging which provides a qualitative assessment of the crystal morphology.

Electron backscattered analysis revealed an abundance of phyllosilicates in these samples (Figs. 4.2a,b, 4.3a), possibly in part reflecting the splitting of the sample chips along, rather than across, the sedimentary laminae. Quartz occurs as individual grains without overgrowths, commonly wrapped by illite or mica grains. Chert was not observed, although it does occur in other samples in minor amounts (Section 3.3).

Element scans produced spectra corresponding to the cations Al, K, Fe, and Si. The chemistry, in conjunction with the observed crystal morphologies, corresponds to minerals such as

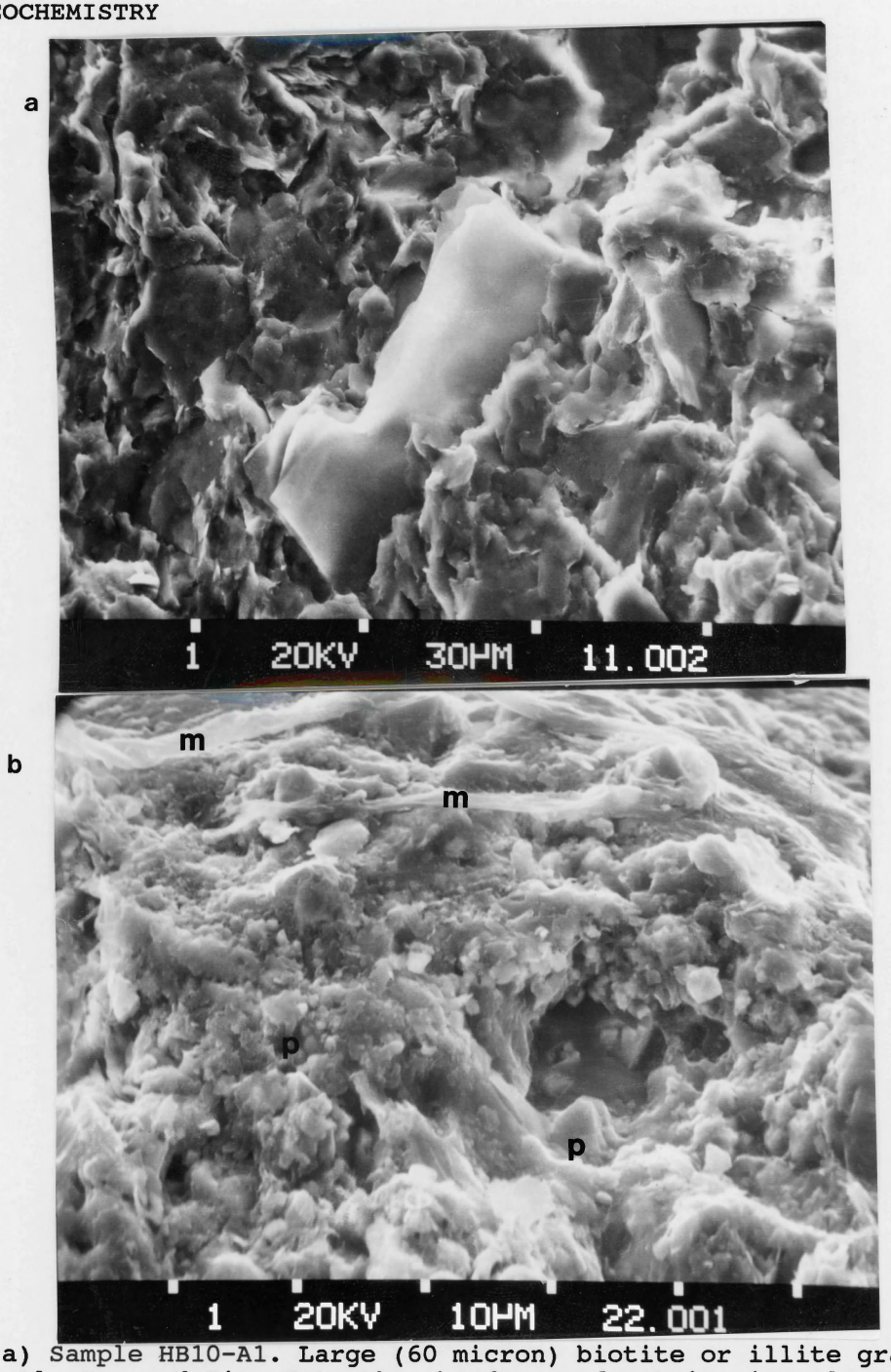

Figure 4.2 a) Sample HB10-A1. Large (60 micron) biotite or illite grain (EDS of K, Al, Fe, and Si). Note the abundance of matrix-size clay in this sample. b) Sample HB10-B2. Micrograph shows elongate muscovite or illite grains (m) (EDS of K, Al, Si) and individual and aggregate pyrite crystals (p). The individual pyrite crystals are approximately 5 microns in diameter although only a protruding corner of each pyrite cube is visible. The number (1) on the bottom left of the micrographs means that a secondary electron detector was used, 20KV is the electron accelerator energy, the third number from the left is the scale of the micrograph (i.e. 10μm = 10 microns between the white squares at the bottom of the picture), and the number on the right is the micrograph photo frame number.

a

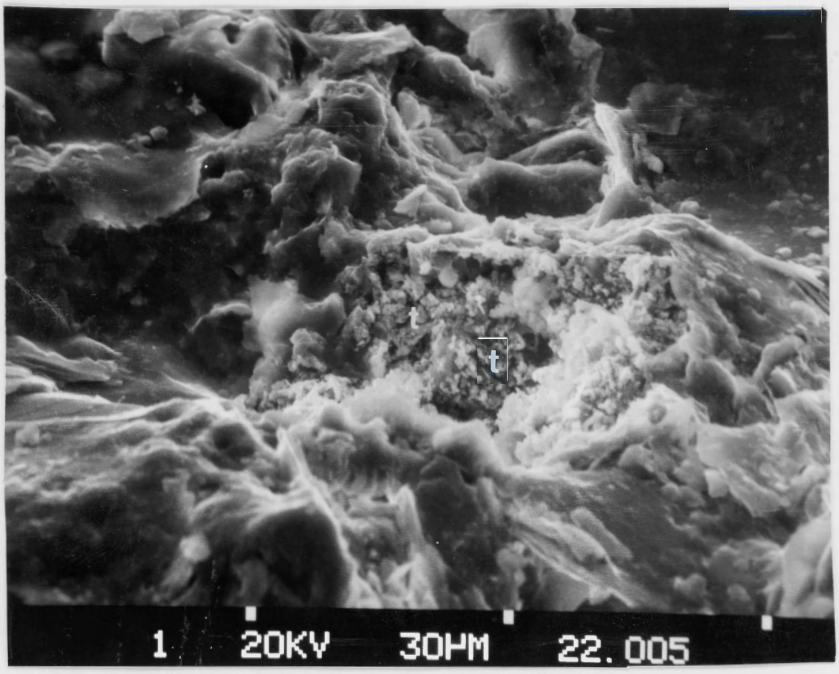

b

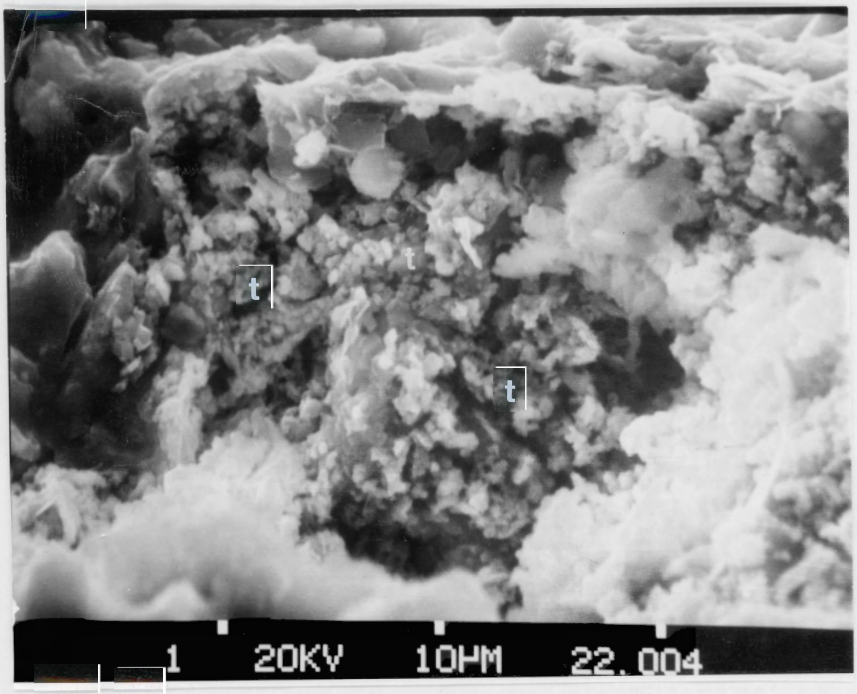

Figure 4.3 a) Sample HB10-B2. In the centre of the photograph is a clot of TiO_2, 20 microns diameter (t), where individual crystals are less than 1 micron diameter. The TiO2 is surrounded by an aluminum silicate, possibly kaolinite. b) Sample HB10-B2. Close-up view of Figure 4.3a. In the centre is TiO_2 clot (t) surrounded by quartz and aluminum-silicate clay.

biotite, muscovite, clay minerals (kaolinite, illite), and quartz. Also common was Ti occurring in rutile, anatase, or brookite (mineral species not determined) as microcrystalline aggregates (Fig. 4.3a,b), and as individual crystals over 20 microns long (Fig. 4.4). Similarly, pyrite occurs as aggregates of small crystals and as individual larger crystals (Fig. 4.2b). Note that the EDS cannot detect elements with an atomic number lower than 8, therefore the complete mineral chemistry is not always given.

4.5 Major and Trace Elements

Table 4.2 contains the major and trace element composition of the sampled profiles as determined by X-ray fluorescence. The average error in analysis was 5-10% for trace elements and 0.5% for major elements, however the error in Th is 51%, rendering the Th analyses unusable. Titanium oxide is high at values of 0.91-1.31%, which corresponds with the ubiquitous titanium revealed in the SEM analysis of four samples (Section 3.2). All of the trace elements lie within the ranges for modern soils reported by Levinson (1974, Table 2-1) and Aubert and Pinta (1977).

4.6 Parent Material Uniformity

A determination of original compositional uniformity must be established for each of the three profiles in order to assess the degree of profile geochemical weathering. A non-uniform parent material may create a misleading soil-horizon profile because

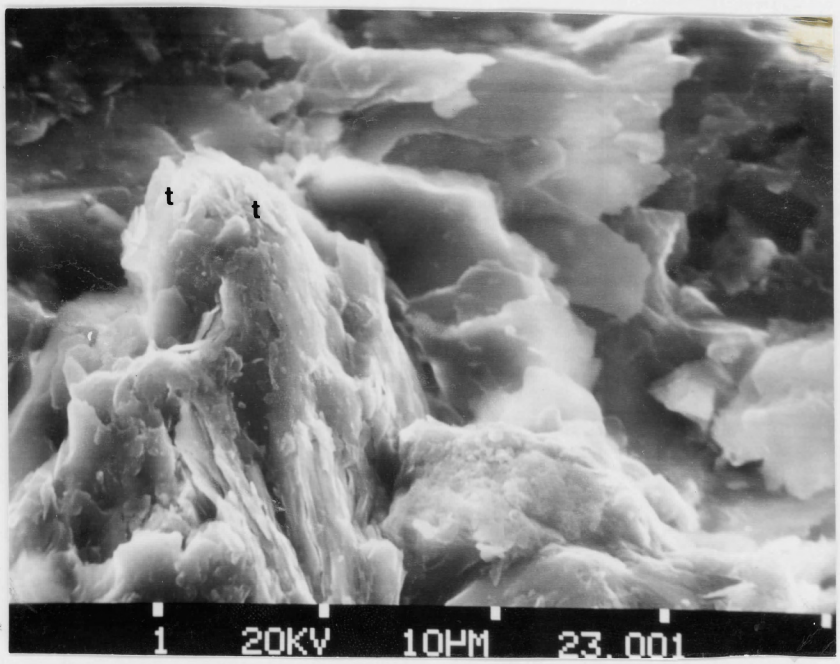

Figure 4.4 Sample HB10-B3. Protruding grain (t) is at least 20 microns long and is composed of virtually pure TiO_2 (rutile/anatase/brookite); it is probably a detrital grain. The TiO2 is surrounded by clay flakes of kaolinite (Al, Si) and illite (K, Al, Si) of approximately the same size as the TiO2 (10-20 microns).

	SiO2	Al2O3	Fe2O3	MgO	CaO	Na2O	K2O	TiO2	MnO	P2O5	L.O.I.
A1	55.42	22.01	8.63	1.68	0.32	0.37	3.78	0.97	0.04	0.03	6.50
A2	68.54	14.06	6.34	0.94	0.51	0.47	2.42	1.08	0.03	0.02	4.60
A3	68.79	16.14	4.72	1.28	0.07	0.46	2.08	1.31	0.11	0.03	5.40
A4	71.20	13.07	5.91	1.31	0.55	0.55	1.84	1.03	0.07	0.02	4.30
B1	55.38	22.82	8.71	1.92	0.09	0.42	3.83	0.91	0.04	0.03	6.40
B2	70.16	15.34	4.04	0.78	0.05	0.46	2.29	1.12	0.02	0.03	4.80
B3	80.06	8.77	2.50	0.52	1.12	0.57	1.05	1.09	0.10	0.05	3.50
B3/1	71.33	14.00	5.34	0.89	0.19	0.50	2.05	1.08	0.03	0.03	3.90
B4	62.11	20.38	6.26	1.39	0.08	0.36	3.24	1.10	0.04	0.03	5.40
B5	58.10	21.40	7.13	1.58	0.10	0.39	3.60	1.02	0.14	0.03	6.00
C4	67.65	15.31	4.18	1.13	0.40	0.42	2.68	1.02	0.02	0.17	6.80
C5	61.52	19.00	5.37	1.58	0.65	0.36	3.50	1.02	0.12	0.08	7.20
C6	66.22	15.73	5.90	1.43	0.37	0.38	2.48	1.10	0.11	0.06	5.40

	Ba	Rb	Sr	Y	Zr	Nb	Th	Pb	Ga	Zn	Cu	Ni	V	Cr
A1	732	181	167	24	171	19	18	22	26	93	76	38	171	141
A2	514	106	96	42	677	21	20	17	17	48	35	26	136	124
A3	602	118	114	29	306	21	19	20	20	95	13	51	129	102
A4	846	88	102	27	295	18	14	11	15	92	19	40	99	93
B1	688	179	160	30	154	17	19	40	31	115	51	44	174	143
B2	447	115	170	38	412	20	15	23	18	53	21	29	117	105
B3	195	48	94	40	677	18	<10	36	10	39	35	18	66	71
B3/1	367	98	107	34	471	20	17	34	16	65	35	39	115	98
B4	632	149	139	34	263	21	19	22	27	94	40	51	147	127
B5	674	163	163	34	204	18	19	25	30	101	38	57	159	138
C4	410	137	156	35	284	19	16	30	21	163	32	46	113	106
C5	489	179	151	34	242	19	22	167	28	117	48	47	154	136
C6	419	118	131	34	325	19	17	22	18	98	31	47	128	112

Table 4.2: Major and trace element data for the three profiles.

characteristics attributed to pedogenesis may actually be inherited from the parent material. For example, a silica-rich soil horizon can form pedogenically, but a similar looking siliceous layer may be merely a slightly reworked sandstone.

Immobile elements (IE's), such as Al, Ti, Y, Ga, Nb, and Zr, can indicate the compositional uniformity of soil parent material (Mason and Moore 1982). Although soils lose many elements from zones of leaching, certain elements form insoluble hydrolysates, and remain in the soil despite weathering processes. Because other material is removed by weathering, the IE's may appear concentrated in the areas where weathering is most intense. However, the ratios of IE's are relatively unaffected by pedogenic weathering, and if a parent material is of uniform composition, the IE ratios should be constant (Muhs et al. 1987).

The varying ratios across the profiles (Table 4.3) reflect the inhomogeneity of the parent material. Generally, the coarser, more silica-rich samples A2 and B3 have relatively high Zr/Y and Zr/Al_2O_3 and low Al_2O_3/TiO_2 ratios, similar to average sandstone ratios (Table 4.3); the reverse is true for the mudstone samples A1, B1, and B5, which correspond to average ratios of shale (Table 4.3). The ratios of profile C lack extreme deviations, therefore profile C formed on a somewhat more homogenous parent sediment. Because the profiles developed on inhomogenous parent material, a weathering trend cannot be determined reliably. reliably. However, the paleosols have high values of TiO_2, Fe_2O_3,

	Zr/Y	Zr/Al2O3	Al_2O_3/TiO_2	Ga/Nb
A1	7.1	7.8	22.7	1.4
A2	16.1	48.2	13.0	0.8
A3	10.6	19.0	12.3	0.9
A4	10.9	22.6	12.7	0.8
B1	5.1	6.8	25.1	1.8
B2	10.8	26.8	13.7	0.9
B3	16.9	77.2	8.0	0.5
B3-1	13.8	33.6	13.0	0.8
B4	7.7	12.9	18.5	1.3
B5	6.0	9.5	21.0	1.7
C4	8.1	18.6	15.0	1.1
C5	7.1	12.7	18.6	1.5
C6	9.6	20.7	14.3	0.9
Ss	14.6	46.0	19.8	–
Sh	6.2	10.4	23.7	1.7

Table 4.3: Immobile element ratios. Ss = sandstone, Sh = shale, ratios of average compositions of sandstone and shale, after Mason and Moore (1982).

and Al_2O_3 and low Na_2O, possibly a result of slight chemical weathering (Faure 1991).

CHAPTER 5 CONCLUSIONS

5.1 Introduction

The span of strata in core HB-10 formed under conditions of a falling base (sea) level, marked by the progression from coal at the base of the core to the red-beds at the top. The three paleosol profiles also reflect this trend. The stratigraphically lowest paleosol (profile C) contains the most organic matter of the three. Although also sub-aqueous and reducing, indicated by grey colour and the presence of pyrite, kutnahorite, and siderite, the profiles A and B contain little organic matter, probably reflecting the drying conditions and a general lack of contemporaneous peat on the floodplain.

5.2 Conclusions

1) Three paleosol profiles studied in the Sydney Mines Formation (Westphalian D) above the Harbour coal seam formed on the tops of coarsening upward lacustrine delta deposits. The profiles are 0.9 to 1.1 m thick; mottled colouring, root traces, incipient horizon development, pyrite, chert, and carbonate concretions, krotovinas, plant fossils, and organic matter identify the strata as paleosols.

2) Paleosol profile A is very weakly developed with well preserved sedimentary layers, profile B is weakly developed with partially erased sedimentary layers, and profile C is moderately developed with good sedimentary mixing and plentiful organic

material in its upper layers. The abundance of relict sedimentary structures and layering indicate that the paleosols are highly immature. This immaturity reflects the brief period available for pedogenesis in a poorly drained environment where sedimentary strata are liable to rapid subsidence and drowning.

3) The grey colour, and the presence of pyrite, siderite, kutnahorite, and organic material indicate the hydromorphic and reducing conditions associated with pedogenesis. Such hydromorphic conditions are consistent with a lacustrine delta setting where sediment bodies rarely build up above the water table.

4) Inconsistent immobile element ratios across the profiles demonstrate the inhomogeneity of parent material. This reflects in part the coarsening upward of the depositional units as the deltas advanced. Pedogenic processes were inadequate to homogenize the parent material before the soils were drowned and buried.

5) Concretions with alternating pyrite and carbonate ($\pm$chert) layers result from fluctuations in ground water pH, a possible result of bacterial respiration. Concretions containing alternating carbonate minerals result from limited cations in diffusive transport. Carbonate and sulphide ions are present in ground water solution, and liberated by bacterial decomposition

of organic matter.

Many, if not all, concretions formed prior to deep burial, as shown in the bedding perpendicular layer of concretions in sample C5, and the concretionary root fill of sample B5.

6) The coarsening up, lacustrine delta units with their immature paleosol profiles are typical of strata directly above the Harbour coal seam, and occupy the basal transgressive part of a cyclothem. Higher strata including red mudstone indicate a basinwide regressive phase and the establishment of a well-drained and oxidising alluvial plain.

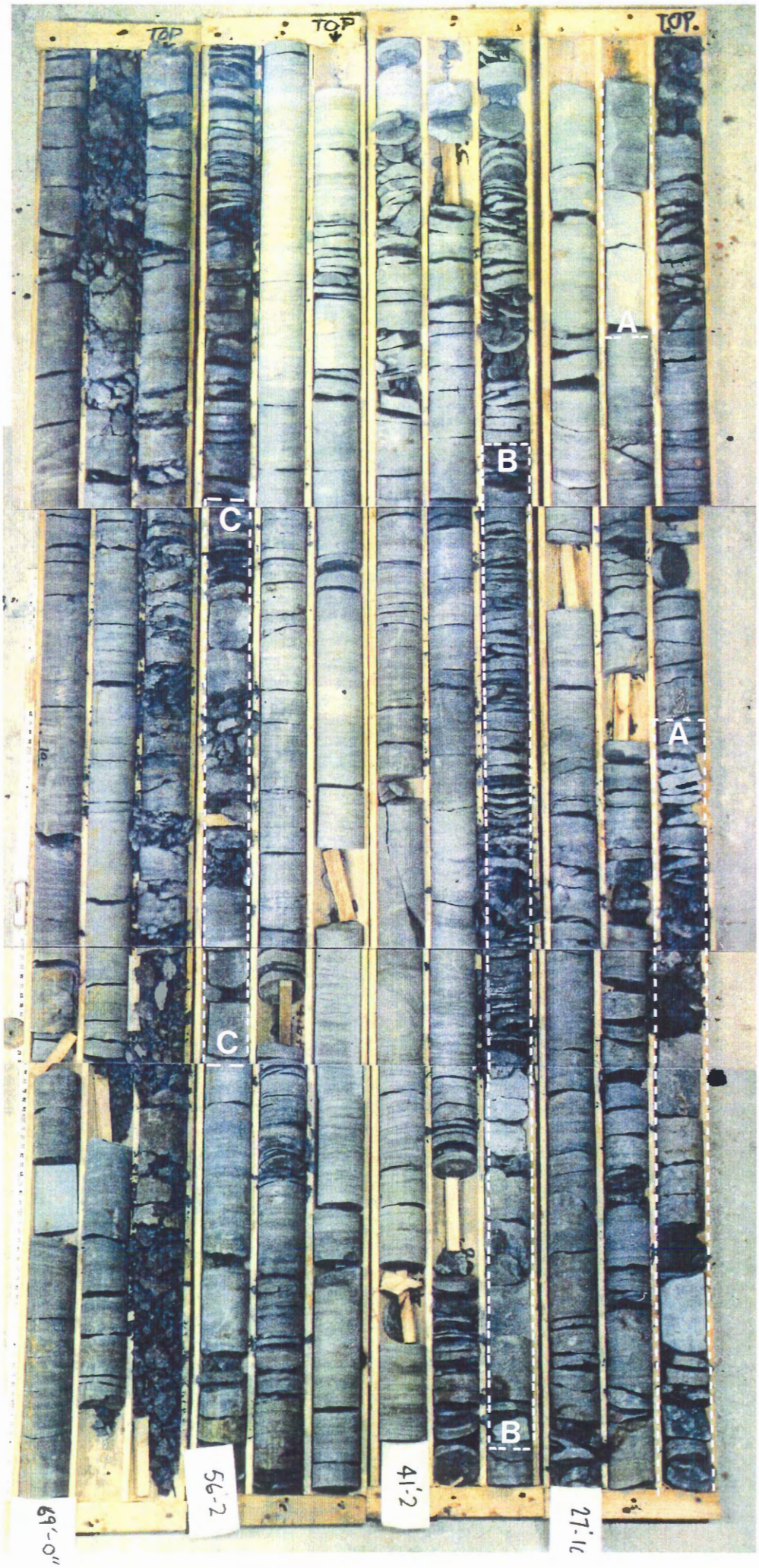
TOP
TOP
TOP
A
B
C
A
C
B
56-2
41'2
27'10
69'-0"

APPENDIX A: INTRODUCTION TO SOIL FEATURES

When pedogenesis (soil-formation) occurs, weathering and organisms destroy primary sedimentary features and replace them with pedogenic features. Discussed below are some of the more common and significant pedogenic features and the processes forming them. Following this discussion is an overview of the large-scale pedogenic features (those visible in hand samples) found in the sampled sections.

Horizons

Soil horizons are layers developed within a soil and are among the most useful diagnostic features of paleosols. Although the horizon sequences vary between and within soil formations, the horizon-forming process is unique to soils. The horizons develop as a result of leaching and sediment mixing. Since the evolution of rooted land-plants in the Late Silurian the dominant soil mixing processes have been root growth and burrowing organisms (Retallack, 1990). Other mixing processes include: percolating ground water; shrinking and swelling of clays (argilliturbation); crystal growth (crystalturbation); gas movement (aeroturbation); and freezing and thawing (cryoturbation)(Allen and Wright, 1989).

Soil horizons are distinguished from regular sediment layers in that the horizons have gradational boundaries and the horizon profile is usually truncated by an erosional upper contact. Soil horizons usually occur in a characteristic sequence of the soil

profile (table 2.1)(Retallack, 1988). Depending on many factors, (parent material, biological activity, weathering conditions, etc.) soil horizon development usually requires 5,000 to 50,000 years to develop (Allen and Wright, 1989).

Glaebules

Glaebules are naturally segregated concentrations of soil material (Brewer, 1964). They range from highly irregular to spherical in shape and form from a wide variety of materials. There are two main types of glaebules: nodules and concretions. A nodule is massive internally, whereas a concretion contains concentric layers. The internal structure depends on the way they form; continuous growth forms nodules, whereas discontinuous (often seasonal) growth forms concretions (Retallack, 1990). Glaebule formation involves chemical precipitation of a mineral. In soils, this can result from many processes, usually involving a change in pH, Eh, chemical precipitation, or bacterial processes. Glaebules often form around a skeleton grain or decomposing organic matter, but they may nucleate wherever conditions are favourable. Generally, the number of glaebules present in a soil is proportional to the degree of pedogenesis, but glaebules proliferate in semi-arid evaporative climates.

Root Traces

One of the best criteria for recognizing a paleosol is root traces. Fossil roots or root traces in a rock are evidence that

plants once grew on the substrate; thus, regardless of its other characteristics, it was once a soil.

The top of a paleosol profile is recognized by the surface from which root traces emanate (certain animal trace fossils such as burrows also descend from surfaces of subaerial exposure). A gradational surface boundary develops if sedimentation continues while plants grow, leading to a cumulate soil (Birkeland 1984).

Root traces differ from other trace fossils because: 1) roots taper and branch downward, 2) roots have irregular widths, and 3) roots often have a concertina-like outline because of compaction of surrounding sediments (Retallack 1990).

Peds and Cutans

Peds are aggregates of soil. They form by accretion of cements, repeated wetting and drying, or coating of soil with films of clay, sesquioxides, and organic matter. Classification of peds is made on the basis of size, angularity, and shape (Retallack 1990)(Fig. 2.1).

Cutans are concentrations of soil material that coat the surfaces of other soil structures. They exist as linings of burrows or root traces, or wrapped around peds, glaebules, and skeleton grains. They vary greatly in composition, which is the basis for their classification (Brewer 1964).

APPENDIX B: GLOSSARY (from Brewer 1964; Wright 1986; Retallack 1990).

Argillasepic Fabric an asepic fabric that consists of mostly anisotropic clay minerals in domains and has a flecked extinction pattern.

Asepic Fabrics Soil fabric with mostly anisotropic plasma, flecked extinction pattern, and no plasma separations. Divided into two subgroups: Argillasepic and silasepic.

Concretion A glaebule with concentric internal structure.

Cutan a concentration of particular soil constituents occurring on or near a surface in the soil such as a crack (plane) or on a rock fragment or glaebule. May be composed of clay (clay cutans, clay skins, or argillans) or calcite (calcan or calcitan) or gibbsite, gypsum, iron oxides, or organic matter. May become fragmented to form papules.

Duricrust Terrestrial material formed within the zone of weathering, in which either iron or aluminum sesquioxides, silica, calcium carbonate, or other materials have accumulated, and may become strongly indurated. Examples include calcrete, silcrete (ganister), and laterites.

Elluviation The removal of soil material from the upper horizons in suspension (lessivage) or solution (leaching). See also illuviation.

Ganister A hard, compact, very fine to medium grained quartz arenite, cemented by authigenic silica dominantly as overgrowths, formed by silica enrichment of a less mature parent material in a paleosol. Ganisters often contain carbonaceous root traces and underlie coal seams (Percival, 1983).

Glaebules A soil feature, recognizeable as a concentration of a mineral or minerals or as having a different fabric than that of the matrix. Nodules are glaebules with no internal structure, concretions have an internal fabric or zoning.

Horizon A layer of soil approximately parallel to the soil surface with characteristics produced by pedogenic processes which distinguish it from other horizons. This is a different usage to that in geology and confusion can result unless this distinction is made when describing paleosols.

Hydromorphic Soils Soils developed in the presence of excess water, typified by gleying and build-up of organic matter.

Illuviation The movement of material from one horizon to another. Usually implies movement of material from an upper horizon to a lower horizon by percolating groundwater or through the burrowing actions of roots or organisms.

Krotovina Also called tounging or glossic features, describes material that illuviates from an upper horizon into a lower horizon, and accumulates in a crack or burrow.

Nodule A glaebule with massive internal structure.

O horizon Organic-matter horizons.

Pedoturbation The mixing of soil by various processes including bioturbation, shrink and swell cycles; does not include illuviation.

Planes Elongate voids in soils; cracks.

Plasma Refers to the part of the soil material which is capable of being moved, concentrated, or reorganized by soil processes. This includes material of colloidal size and soluble material. Really the matrix of a soil, plasma surrounds soil stuctures, skeleton grains, and voids.

Sepic Fabrics Plasmic fabrics in which patches or zones of plasma have striated extinction patterns in crossed polar transmitted light. Various types are recognized.

Silasepic Fabric Soil fabric with highly variable grain sizes and high proportions of silt size grains so that domains are difficult to recognize, matrix has a flecked extinction pattern.

Silcrete a variety of duricrust composed of silica.

Skelsepic Fabric a sepic fabric in which part of the plasma has a flecked extinction, but striated plasma separations are parallel to the surfaces of skeleton grains.

APPENDIX C: STAGES OF SOIL DEVELOPMENT (Retallack 1990)

Very Weakly Developed: Little evidence of soil development, apart from root traces: abundant sedimentary, metamorphic, or igneous textures remaining from parent material.

Weakly Developed: With a surface rooted zone (A-horizon) as well as incipient subsurface clayey, calcareous, sesquioxidic or humic, or surface organic horizons.

Moderately Developed: With surface rooted zone and obvious subsurface clayey, sesquioxidic, humic or calcareous or surface organic horizons.

Strongly Developed: With especially thick, red, clayey or humic subsurface (B) horizons or surface organic horizons (coals and lignites) or especially well developed soil structure or calcic horizons.

Very Strongly Developed: Unusually thick subsurface (B) horizons or surface organic horizons (coals or lignites) or calcic horizons, such a degree of development is mostly found at major geological unconformities.

APPENDIX D: THIN SECTION PETROGRAPHY

Sample percentages based on 200 point counts. Matrix is grains <30 microns. ppl = plane polarized light, xn = cross nichols.

HB10-A1
Matrix: (77%) exhibits argillasepic plasmic fabric with occasional skelsepic around larger grains and concretions. Composed of quartz, feldspar, mica (which show a rough alignment) and indeterminate grains.
Carbonate Glaebules: (23%) some display radial structure, in one area nodules concentrate to form a 2 mm - wide trail.

HB10-A2 (polished section)
Matrix: (71%) shows skelsepic texture around carbonate nodules.
Carbonate Nodules: (20%) brown
Quartz and Feldspar: (9%)

HB10-A3
Matrix: (83%) Domains show lattisepic and argillasepic plasmic fabric.
Quartz and Feldspar: (11%) up to 0.1 mm diameter
Mica: (4%) biotite and white mica.
Pyrite: (2%) 1.5 mm
Carbonate Concretions: (<1%) up to 0.8 mm, concretions show vug type filling on the edges with larger, randomly oriented crystals in the centre.

HB10-A4
Matrix: (50%) Skelattimasepic and argillasepic plasmic fabric. (Plasma grains wrap around quartz, feldspar, pyrite, and carbonate nodules, also forms boxwork and the domains occur in subparallel elongate striated zones.)
Quartz and Feldspar: (32%)
Mica: (13%)
Pyrite: (4%)
Carbonate concretions: (1%) with diffuse edges that grow into the matrix, 3-7 mm diameter, and white centres and brown edges.

HB10-B1
Matrix (100%) Displays lattimosepic and insepic plasmic fabric. In ppl the domains are alternating layers of brown and light brown.

HB10-B2
Matrix: (72%) Quartz, mica, and fine organic material. Features skelsepic plasmic fabric.
Quartz and Feldspar: (20%) average size 0.06 mm, quartz is angular, feldspars are more rounded. Many grains have

undulose extinction patterns, there are very few quartz-quartz contacts (grains are supported by a mica-rich matrix).

Mica: (3%)
Pyrite: (3%) Occurs in clusters of small grains.
Organic: (2%) Black (carbon-rich) and amorphous, often occurs in large (1 mm) pieces. Most is located in elongate root structures.

Root traces show typical tapering and excellent krotovina development. The root trace centres contain much organic material (and other very fine-grained material) which is surrounded by a layer of very fine material free of organics (argillan). The outside of the root trace is a layer of coarser grains.

HB10-B3
Quartz and Feldspar: (51%) grains of 0.1 mm, feldspars have a cloudy surface texture, some quartz grains have sutured contacts, equally as many have matrix supported contacts.
Matrix: (41%) Displays skelsepic plasmic fabric.
Mica: (7%)
Pyrite: (1%)

This slide has one large (5 mm) root trace which has a very fine-grained krotovina centre surrounded by coarser clasts and fine matrix.

HB10-B3-1
Matrix: (49%) skelsepic plasmic fabric
Quartz and Feldspar: (41%) grains ca. 0.1 mm
Mica: (10%)

HB10-B4
Matrix: (63%) Argillasepic plasmic fabric
Quartz and Feldspar: (29%) ca. 0.1 mm
Mica: (7%)
Pyrite: (1%) fine-grained disseminated

This slide has two very large root traces comprising 40% of the slide face. The very fine grained matrix surrounds the root traces which contain coarse (0.1 mm) material. There are small patches of chert (quartz grains of 2.5 microns)

HB10-B5
Matrix: (70%) Mosepic plasmic fabric. Displays small patches of chert in root trace.
Carbonate: (19%)(28% including matrix sized material) Forms as up to 0.4 mm brown nodules and ca. 0.4 mm white concretions. The white concretions display a sheath extinction pattern.
Pyrite:(10%) one large (7 mm) piece of pyrite that is surrounded by abundant brown carbonate nodules, as well as inside root trace where it is found with white carbonate in layered

concretions.
Quartz: (1%) 0.05-0.1 mm grains.

HB10-C2
Matrix: (60%) Mostly organic material, some mica and quartz.
Shell Fragments: (30%) Broken shells, fish vertebrae, ostracods.
Quartz: (10%) Up to 0.15 mm diameter.

HB10-C3
Indistinguishable mineralogy except for quartz crystals and shells (5%). This sample has well defined layering, contains 80% organic material.

HB10-C4
Matrix: (99%) contains quartz, feldspar, mica, and organic material. Displays argillasepic plasmic fabric

This sample has large (1 cm) root structures and quartz patches with crystals ca. 2.5 microns dia. possibly from diagenetic decomposition of feldspar. This sample is very well mixed, any former layering is obliterated.

HB10-C5
A very fragile sample, as a result, grinding of the thin section left only two large (≈1 cm dia) carbonate nodule patches. One patch is round, the other elongate, both contain carbonate, pyrite, quartz, and small amounts of mica.

Carbonate: (95%) white and brown, occur as separate nodules but also together in a honeycomb structure where nodules are separated by bands of pyrite.

Pyrite: (4%) occurs in nodular form and also interspersed with carbonate nodules.

Quartz: (1%) individual grains are up to 0.1 mm, also mats (0.5 mm) of chert (5 micron crystals) possibly from the diagenetic decomposition of clay minerals.

HB10-C6
Matrix: (70.6%) exhibits argillasepic plasmic fabric.
Quartz and Feldspar: (15.5%) Grains are ≈ 0.12 mm, very few point-point contacts, mostly surrounded by mica.
Mica: (10.3%) up to 0.2 mm.
Pyrite: (3.4%) occurs as individual grains and in patches of many grains.

APPENDIX E: SPECIFICATIONS FOR ANALYTICAL TOOLS

Electron Microprobe, model JEOL 733 Superprobe, is located at Dalhousie University. It operates in the WDS mode, four wavelength spectrometer, with operating conditions of 15 keV at 10 nanoamps, using geological standards. Tracor-Northern ZAF matrix correction program. Error is estimated to be $\pm$ 1.5 - 2.0%.

Scanning Electron Microscope, at Bedford Institute of Oceanography, is a Cambridge Instruments model S-180, with EG and G Ortec X-ray dispersive (EDS) spectrometer (model EEGS-II), secondary electron analyser, with a 20 keV accelerator. No error was measured as the SEM was used for qualitative analyses only.

X-Ray Fluorescence, a Philips PW 1400 sequential X-ray fluorescence spectrometer, located at Saint Mary's University, uses an RH-anode X-ray tube, and is calibrated with geological standards. The trace elements are analyzed on pressed powder pellets. Average error = 5-10% for trace elements, and less than 0.5% for major elements.

REFERENCES

Allen JRL, (1974) Studies in fluviatile sedimentation: implications of pedogenic carbonate units, Lower Old Red Sandstone, Anglo-Welsh outcrop. Geol Jour 9:181-208.

Allen JRL, Wright VP (1989) Paleosols in Siliclastic Sequences, PRIS Short Course Notes No. 001, Reading University, Whiteknights, Reading, 97 pp.

Aubert H, Pinta M (1977) Trace Elements in Soils. Developments in Soil Science, 7. Elsevier, Amsterdam, 395 pp.

Barnaby RJ, Rimstidt JD (1989) Redox conditions of calcite cementation interpreted from Mn and Fe contents of authigenic calcites. GSA Bull 101:795-804.

Berner RA (1981) Early diagenesis: A theoretical approach. Princeton series in geochemistry. Princeton University Press, Princeton N.J., 241 pp.

Berry LG, Mason BH, Dietrich RV (1983) Mineralogy. Freeman and Co., Kingsport, Tennessee, 561 pp.

Birkeland PW (1984) Soils and geomorphology, Oxford University Press, New York, 315 pp.

Boehner RC, Giles PS (1986) Geological map of the Sydney Basin. Nova Scotia Department of Mines and Energy, map 86-1.

Brewer R (1964) Fabric and mineral analysis of soils. Wiley, New York, 470 pp.

Buringh P (1970) Introduction to the study of soils in tropical and subtropical regions. Wageningen Centre for Agricultural Publishing and Documentation, Netherlands, 99 pp.

Catt J (1990)(ed) Paleopedology manual. Quat Int 6:1-95.

Dana JD, Dana ES (1952) The System of Mineralogy, Vol. 2. 7th ed., Wiley, New York.

Faure G (1991) Principles and applications of inorganic geochemistry. Macmillan, New York. 626 pp.

Foth HD (1984) Fundamentals of Soil Science. Wiley, New York. 435 pp.

Gibling MR (1991) Sequence analysis of alluvial-dominated cyclothems in the Sydney basin, Nova Scotia.

Gibling MR, Rust BR (1990) Ribbon sandstones in the Pennsylvanian Waddens Cove Formation, Sydney Basin, Atlantic Canada: the influence of siliceous duricrusts on channel-body geometry. Sedimen 37:45-65.

Gibling MR, Rust BR (in press) Silica cemented paleosols (Ganisters) in the Pennsylvanian Waddens Cove Formation, Nova Scotia, Canada. In: Diagenesis. Chilingarian GV, Wolf KH (eds) Elsevier, Amsterdam.

Hacquebard PA (1983) Geological development and economic potential of the Sydney coal basin, Nova Scotia. In: Current research, part A, G.S.C. paper 83-1A, pp71-81.

Kraus MJ, Bown TM (1986) Paleosols and time resolution in alluvial stratigraphy. In: Wright VP (ed) Paleosols: Their recognition and interpretation, Princeton University Press, Princeton, N.J., 315 pp.

Krumbein WC, Garrels RM (1952) Origin and classification of chemical sediments in terms of pH and oxidation-reduction potentials. Jour Geol 60:1-33.

Leckie D, Fox C, Tarnocai C (1989) Multiple paleosols of the late Albian Boulder Creek Formation, British Columbia, Canada. Sedimen 36:307-323.

Levinson AA (1974) Introduction to Exploration Geochemistry. Applied, Maywood, Ill., 614 pp.

Marshall CE (1977) The Physical Chemistry and Mineralogy of Soils, Vol.2, soils in place, John Wiley, Toronto, 313 pp.

Mason BH, Moore CB (1982) Principles of Geochemistry, fourth ed. Wiley, New York, 344 pp.

Masson AG, Rust BR (1983) Lacustrine stromatolites and algal laminites in a Pennsylvanian coal-bearing succession near Sydney, Nova Scotia, Canada. Can Jour E Sci 20:1111-1118.

Masson AG, Rust BR (1984) Fresh-water shark teeth as paleoenvironment indicators in the upper Pennsylvanian Morien Group of the Sydney Basin, Nova Scotia. Can Jour E Sci 21:1151-1155.

Masson AG, Rust BR (1990) Alluvial plain sedimentation in the Pennsylvanian Sydney mines Formation, eastern Sydney Basin, Nova Scotia. Bull Can Pet Geol 38:89-105.

McFarlane MJ (1983) Laterites. In Chemical Sediments and Geomorphology. Goudie AS, Pye K (eds) Academic Press, London, pp7-58.

Monger HC, LeRoy AD, Lindemann WC, and Liddell CM (1991) Microbial precipitation of pedogenic calcite. Geol 19:997-1000.

Muhs DR, Crittenden RC, Rosholt JN, Bush CA, Stewart KC (1987) Genesis of marine terrace soils, Barbados, West Indies: Evidence from mineralogy and geochemistry. E Surf Proc Land 12:605-618.

Percival CJ (1983) A definition of the term ganister. Geol Mag 120:187-190.

Powers MC (1953) A new roundness scale for sedimentary particles. Jour Sed Pet 23:117-119.

Retallack GJ (1988) Field recognition of paleosols. G.S.A. Sp Paper 216:1-20.

Retallack GJ (1990) Soils of the past, an introduction to paleopedology. Unwin Hyman, Boston, 520 pp.

Rust BR, Gibling MR, Best MA, Dilles SJ, Masson AG (1987) A sedimentological overview of the coal-bearing Morien Group (Pennsylvanian) Sydney Basin, Nova Scotia, Canada. Can Jour E Sci. 24:1869-1885.

Ryan RJ, Calder JH, Donohoe HV Jr, and Naylor R, (1987) Late Paleozoic sedimentation and basin development adjacent to the Cobequid Highlands Massif, eastern Canada. In Beaumont C, Tankard AJ (eds) Sedimentary basins and basin forming mechanisms. Can Soc Pet Geol, Memoir 12. pp299-309.

Sehgal JL, Stoops G (1972) Pedogenic calcic accumulations in arid and semi-arid regions of the Indo-Gangetic alluvial plain of the erstwhile Punjab (India), their morpholgy and origin. Geoderma 8:59-72.

Tye RS, Coleman JM (1989) Depositional processes and stratigraphy of fluvially dominated lacustrine deltas: Mississippi delta plain. Jour Sed Pet 59:973-996.

Valentine, K.W.G., and Dalrymple, J.B., 1976. Quaternary buried paleosols; a critical review. Quat Res 6:209-220.

Walker RG, Cant DJ (1989) Sandy fluvial systems. In: Walker RJ (ed) Facies models. 2nd ed, Geoscience Canada, Reprint series 1. pp71-89.

Wightman WG, Scott DB, Gibling MR (1992) Upper Pennsylvanian agglutinated foraminifers from the Cape Breton coalfield, Nova Scotia: Their use in determination of brackish-marine depositional environments. Abstr G.A.C Meet.

Wilkinson M (1989) Evidence for surface reaction-controlled growth of carbonate concretions in shales. Sed 36:951-953.

Wright VP (1986) Paleosols: Their recognition and interpretation. Princeton University Press, Princeton, N.J., 315 pp.

Wright VP (1988) A genetic classification of ancient and modern calcretes based on microstructure. Abstr Int Assoc Sed Eur Reg Meet pp225-226.

Wright VP (1989) A micromorphological classification of calcretes. Proc VII Int Wkg Meet Soil Micro.

Yaalon D (1990) The relevance of soils and paleosols in interpreting past and ongoing climatic changes. Palaeogeo Palaeoclima, Palaeoeco 82:63-64.